No. 2 1973

issued quarterly

Technical Review

To Advance Techniques in Acoustical, Electrical and Mechanical Measurement

High Speed Analysis Bone Conduction Noise Screens

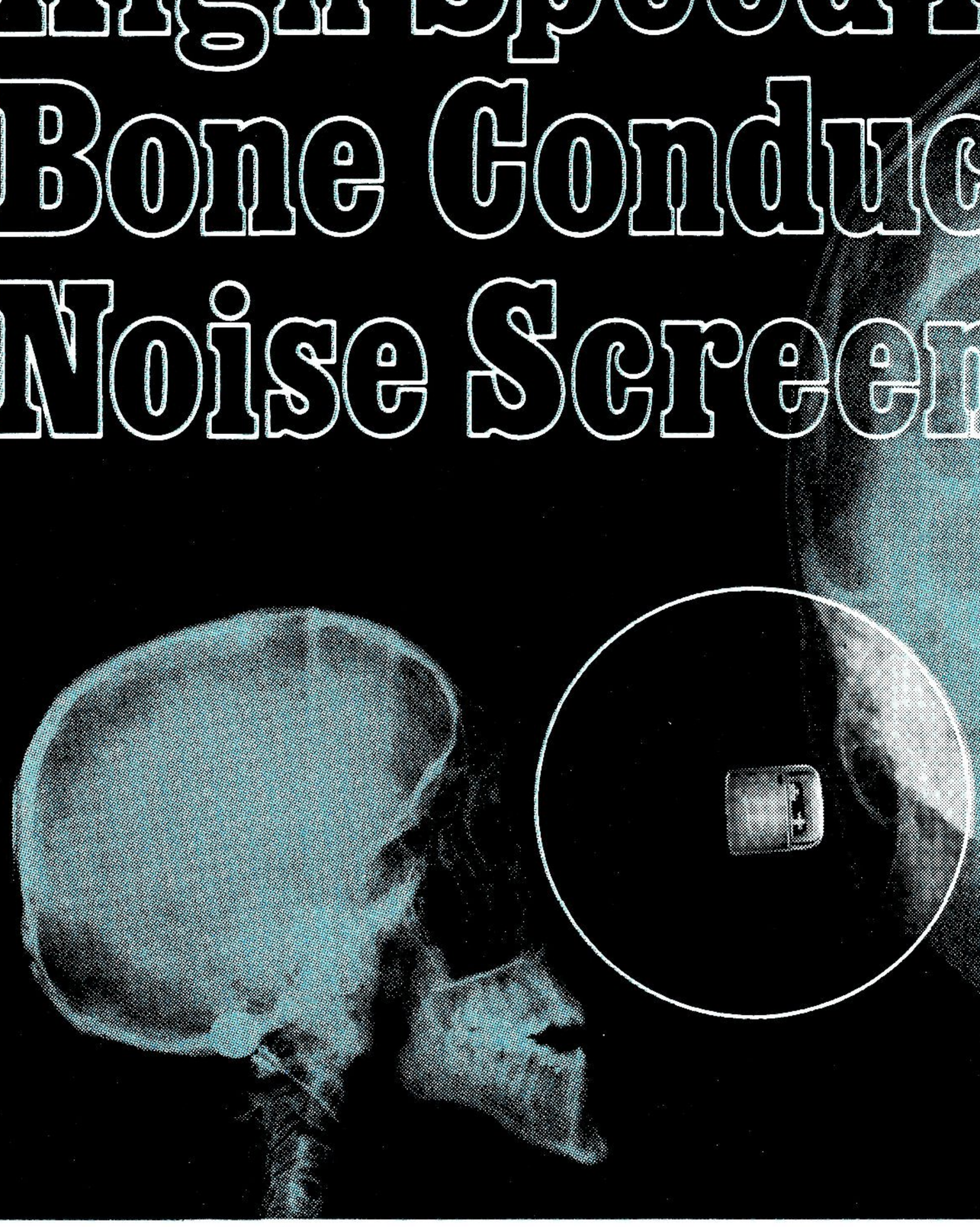

BRÜEL & KJÆR

PREVIOUSLY ISSUED NUMBERS OF BRÜEL & KJÆR TECHNICAL REVIEW

1–1973 Calibration of Hydrophones.
The Measurement of Reverberation Characteristics.
Adaptation of Frequency Analyzer Type 2107 to Automated 1/12 Octave Spectrum Analysis in Musical Acoustics.
Bekesy Audiometry with Standard Equipment.

4–1972 Measurement of Elastic Modulus and Loss Factor of Asphalt.
The Digital Event Recorder Type 7502.
Determination of the Radii of Nodal Circles on a Circular Metal Plate.
New Protractor for Reverberation Time Measurements.

3–1972 Thermal Noise in Microphones and Preamplifiers.
High Frequency Response of Force Transducers.
Measurement of Low Level Vibrations in Buildings.
Measurement of Damping Factor Using the Resonance Method.

2–1972 RMS-Rectifiers.
Scandinavian Efforts to Standardize Acoustic.
Response in Theaters and Dubbing Rooms.
Noise Dose Measurements.

1–1972 Loudness Evaluation of Acoustic Impulses.
Computer Programming Requirements for Acoustic Measurements.
Computer Interface and Software for On-Line Evaluation of Noise Data.
Evaluation of Noise Measurements in Algol-60.

4–1971 Application of Electro-Acoustical Techniques to the Determination of the Modulus of Elasticity by a Non-Destructive Process.
Estimation of Sound Pressure Levels at a Distance from a Noise Source.
Acoustical Calibrator Type 4230 and its Equivalent Diagram.

3–1971 Conventional & On-line Methods of Sound Power Measurements.
An Experimental Channel Selector System.

2–1971 Interchangeable Head Vibration Exiters.
AEROS: A Generalized-Spectrum Vibration-Control System.

1–1971 Shock and Vibration Isolation of a Punch Press.
Vibration Measurement by a Laser Interferometer.
A portable Calibrator for Accelerometers.
Electro Acoustic Ear Impedance Indicator for Medical Diagnosis.

(Continued on cover page 3)

TECHNICAL REVIEW

No. 2 — 1973

Contents

Front cover picture:

The front cover picture illustrates the application of a bone vibrator to the human mastoid. Thanks are due to the Royal Dental College, Copenhagen for their kind assistance in obtaining the x-ray photos. Thanks are also due to Oticon A/S, Copenhagen for their permission to use one of their new bone vibrators for this purpose.

High Speed Narrow Band Analysis using the Digital Event Recorder Type 7502

by

R.B. Randall, B. Tech., B.A.

ABSTRACT

The paper discusses the means for reduction of the relatively long analysis time in normal narrow band swept frequency analysis. One useful method is to repeat a sample of the signal continuously at a high speed for fast analysis. This can be carried out with a tape recorder, but the Digital Event Recorder is to be preferred because of the large speed transformations available and since it eliminates splicing problems.

The paper points to the problem of sidebands which are produced when a signal sample is continuously repeated. In practice, the sidebands can limit the selectivity of the analysis and graphs are given for determination of this effect, where highly selective filters are used. The effect can however be made negligible by introducing a smoothly contoured weighting function which eliminates the signal discontinuities at the sample ends.

Examples are given of typical savings in analysis time.

SOMMAIRE

L'article discute les moyens permettant de réduire le temps d'analyse relativement long des analyses normales en bande étroite balayée. Une méthode intéressante consiste à répéter continuellement un échantillon du signal à une vitesse plus élevée pour obtenir une analyse rapide. On peut utiliser pour cela un enregistreur magnétique mais l'Enregistreur Numérique est préférable car il offre de grandes possibilités de transformation de vitesse et il élimine les problèmes de jonction de bande.

L'article souligne le problème des bandes latérales produites lorsqu'un échantillon de signal est continuellement répété. Elles réduisent en pratique la résolution de l'analyse et on donne des courbes pour déterminer cet effet lorsqu'on utilise des filtres hautement sélectifs. On peut toutefois rendre cet effet négligeable en introduisant une fonction de pondération au contours régulier qui élimine les discontinuités aux extrémités de l'échantillon.

On donne aussi des exemples de gains sur le temps d'analyse.

ZUSAMMENFASSUNG

Es werden Hilfsmittel zur Verminderung der relativ langen Analysierdauer bei einer normalen Schmalbandanalyse mit stetiger Filterdurchstimmung diskutiert. Eine zweckmäßige Methode

ist die ständige Wiederholung eines Signalausschnitts mit hoher Geschwindigkeit für eine schnelle Analyse. Dies läßt sich mit einem Bandgerät ausführen, dem jedoch ein digitaler Signalspeicher vorzuziehen ist wegen der großen erzielbaren Geschwindigkeitstransformation und weil mechniasche Bandstoßprobleme entfallen.

Ferner wird das Problem der Seitenbänder behandelt, die durch die Unstetigkeiten bei der ständigen Wiederholung eines Signalausschnitts verursacht werden. In der Praxis können diese Seitenbänder die Selektivität der Analyse begrenzen, und es werden Diagramme angegeben zur Bestimmung dieses Effekts, wenn hochselektive Filter benutzt werden. Der Effekt läßt sich jedoch vernachlässigbar klein machen durch zeitliche Bewertung mit einer abgerundeten Fensterfunktion, welche die Unstetigkeiten an den Nahtstellen des Signals unterdrückt.

Typische Beispiele für die Einsparung an Analysierzeit werden angegeben.

Introduction

Narrow band frequency analysis is normally carried out either by relatively slow swept frequency techniques or by very fast "real-time" frequency analysis. There are some applications where the real-time aspect of the latter technique is itself an advantage (e.g. when the effects of changing conditions are to be followed visually).

In other cases however, the important aspect is the analysis time, and it can be a considerable advantage to reduce this down to a few minutes from what may be an hour or more.

Such a reduction is often made possible by means of the Digital Event Recorder Type 7502, which has an extremely wide range of ratios of play-back to recording speed. Although as its name implies it was originally designed to replace a magnetic tape loop in the recording and analysis of single events and impulses, it can also be used for the analysis of continuous signals provided certain precautions are taken. This paper gives a guide to some of the most important factors to be taken into account, and demonstrates the savings in analysis time which can be made.

Further reduction of analysis time than indicated above may not give much advantage, in consideration of the time required to set up each analysis and obtain a "hard" copy of the results on a level recorder.

Time Compression Analysis

If a sample of a signal is recorded and played back at a higher speed, this theoretically allows a reduction in analysis time proportional to the speed increase. This can be explained as follows. A speed-up by a factor of for example 100:1 increases the frequency range to be covered by a

factor of 100:1 but for the same resolution, allows an increase of analyzer bandwidth by 100:1.

In terms of the recording on paper, the same paper length can be used to represent the analysis range, and the analyzer bandwidth will then still represent the same length along the paper. However, the required dwell time per bandwidth (T_D) in a swept frequency analysis is governed by expressions of the form BT_D = constant, and can thus be reduced in proportion to the increase in bandwidth (Ref.3). Sweeping one bandwidth per dwell time thus results in an increase of paper speed and a decrease of total analysis time in the same proportion.

It is not always possible to make full use of this theoretical improvement as shown later, but even with some inefficiency a significant reduction of analysis time can normally be obtained.

In practice it is generally necessary to join a signal sample into a loop for repetitive playback at the higher speed, and the effects of this should be examined.

Analysis of a Looped Signal

When a sample is taken of a continuous signal and joined into a loop for playback, as in the case of the 7502 (or with a tape recorder) this can give rise to problems at the junction point. Only those frequency components which have exactly an integral number of periods along the loop will be represented truly as continuous sinusoids. For all others, there will be a discontinuity at the junction which gives rise to spurious components not present in the original signal. One way of overcoming this problem is to multiply the sample by a smoothly contoured weighting function, or "time window", which has a value of zero at the discontinuity and thus nullifies its effect. (See Fig.1 which shows a signal sample multiplied with a gaussian impulse from the Gauss Impulse Multiplier Type 5623).

When no special weighting function is employed the signal can be considered as multiplied by a rectangular time window which has the same length as the sample. The effect of this can be calculated and a judgement made of the necessity to employ a special window function.

Considering first one loop length in isolation, the multiplication of the time signal by a window function results in a convolution of their respective Fourier transforms in the frequency domain (Ref. 1). The effect of this for a sinusoidal input is illustrated in Fig.2.

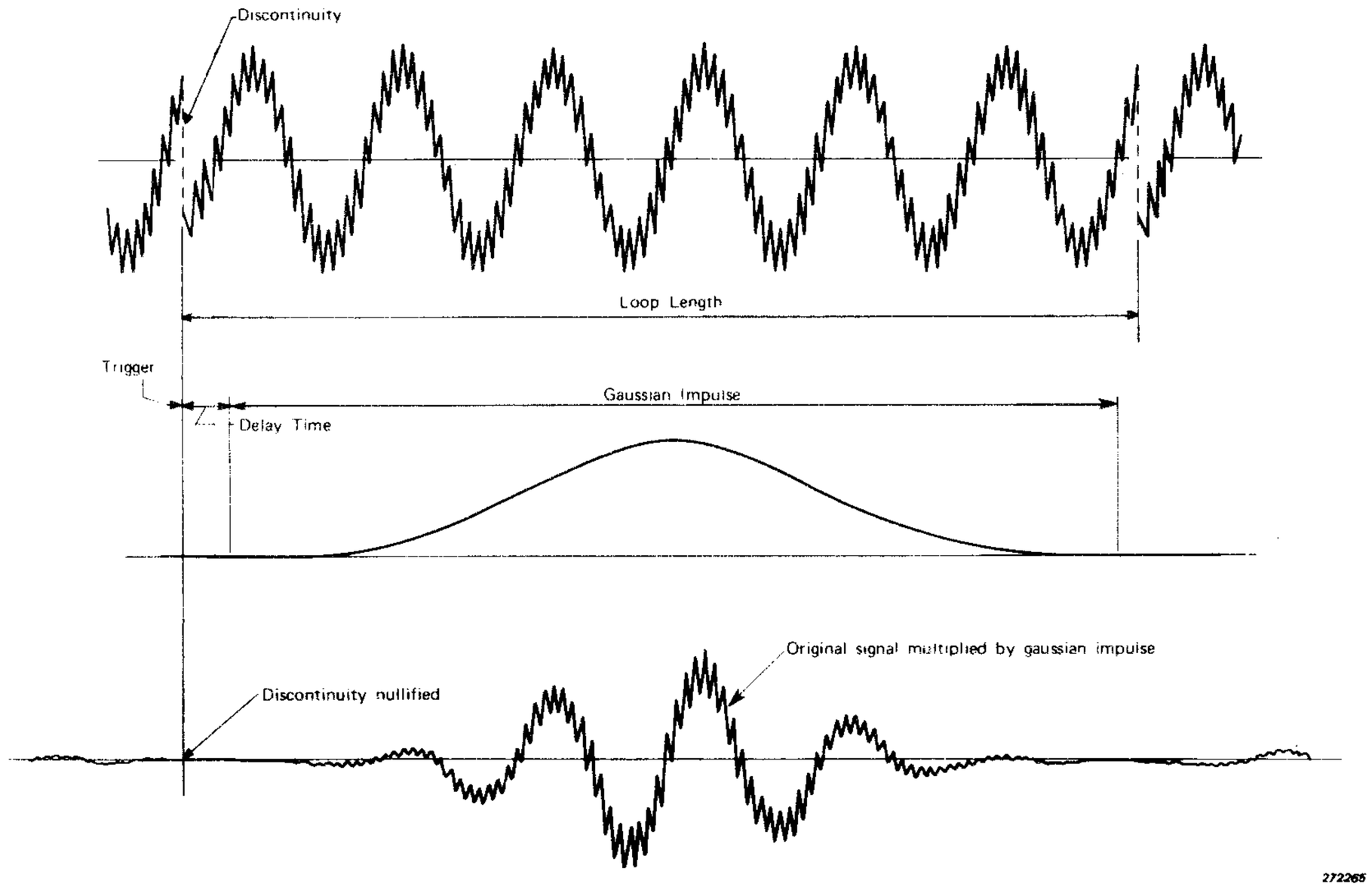

Fig. 1. Effect on Signal Discontinuity of Gaussian Time Window

Fig. 2a shows a sinusoidal signal p(t) of infinite extent and its (2-sided) spectrum in the frequency domain P(f) which in fact is a pair of spectral lines (delta functions) situated at $\pm f_o$ the frequency of the sinewave (Ref. 1). The (1-sided) spectrum obtained by passing an ideal filter of bandwidth B across this true spectrum is also shown. Note that the two spectra have been drawn to logarithmic amplitude scales but linear frequency scales. This representation is identical for the amplitude of the Fourier spectrum (disregarding phase) and for the power spectrum.

Fig. 2b shows the power spectrum of a rectangular window q(t) of length T illustrating the extent of the sidelobes obtained in the Fourier spectrum Q(f), which is the well-known sin x/x function with sidelobe width 1/T.

Fig. 2c shows the effect of multiplying the original infinite signal p(t) by the rectangular window q(t). This results in the convolution P(f) * Q(f) in the frequency domain, which can be interpreted simply as filtering the original spectrum P(f) with a sweeping filter of shape Q(f). (See Appendis A). The further convolution obtained by sweeping an ideal filter across the resulting spectrum is also shown.

Figs. 2d and 2e show the analogous results obtained with a gaussian window.

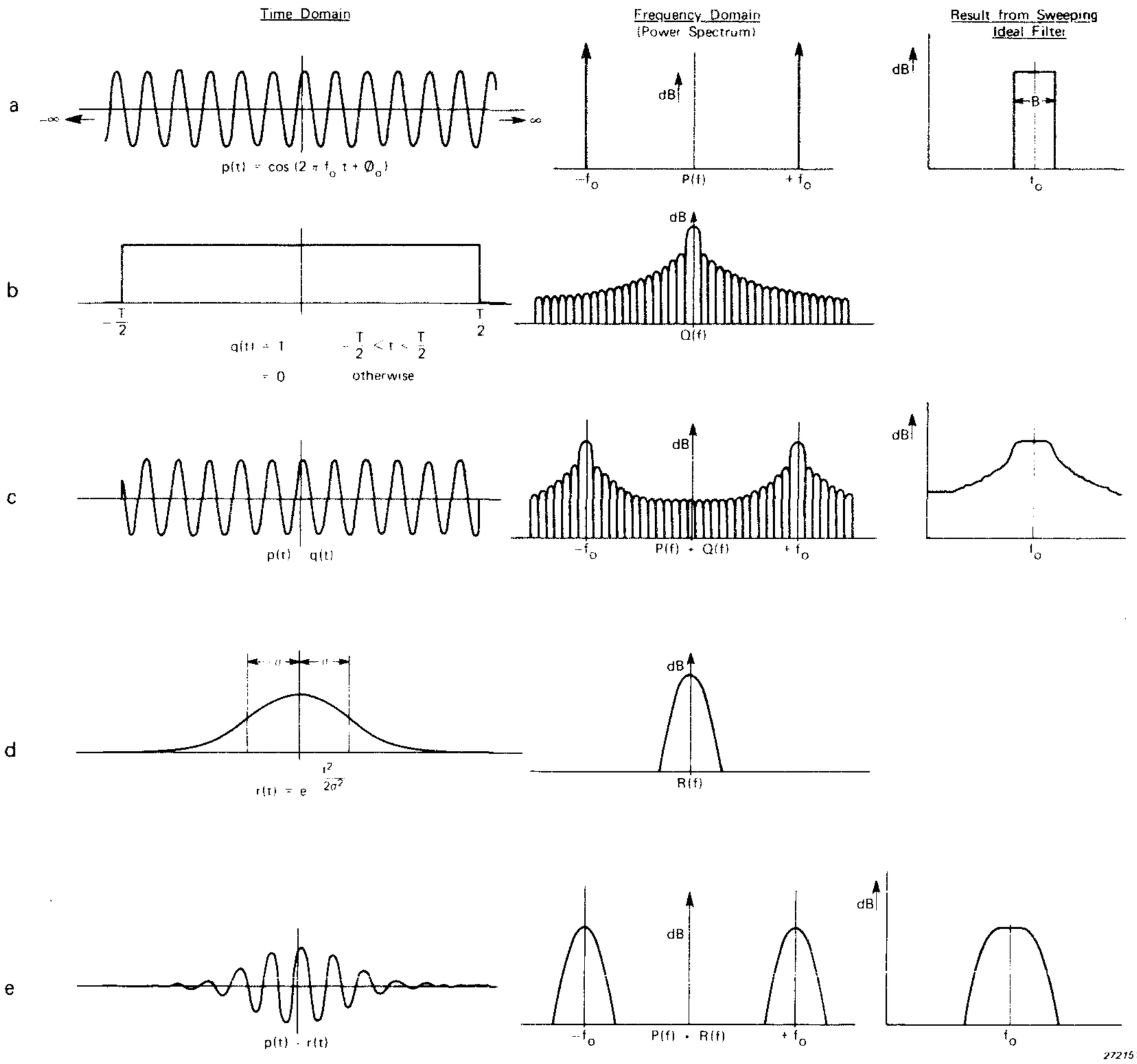

Fig.2. Comparison of Rectangular and Gaussian Window in Time and Frequency Domains

The overall characteristic with which the original signal is filtered is thus the convolution of the Fourier transformed window function with the Fourier spectrum of the analysing filter.

So far the windowed function has been considered in isolation. If it is now joined into a loop of length T_r seconds and played back continuously, the result is a periodic function which has a line spectrum as opposed to the continuous spectrum illustrated in Fig.2. The line spectrum can be determined from the continuous spectrum, however, by sampling it at frequency intervals of $1/T_r$ Hz. (Ref. 2). For the particular case of a rectangular window of length T secs. the resulting sidelobes in the frequency domain are of width $1/T$ Hz. (Ref. 2). A very interesting result is obtained in the limit as T approaches T_r (the case represented by a simple looped signal) since then the Fourier line spacing is equal to the sidelobe width, and the spectrum is thus sampled once per sidelobe.

What effect this has depends on where the sidelobes are sampled, and Fig.3 illustrates the extreme possibilities represented by sampling

(a) at the peaks of the sidelobes
(b) at the zero points between the sidelobes.

It will be found that (b) corresponds to the cases where there is an integer number of periods along the loop, since the resulting signal is indistinguishable from a continuous sinewave and thus has only one component, as illustrated in Fig.3.

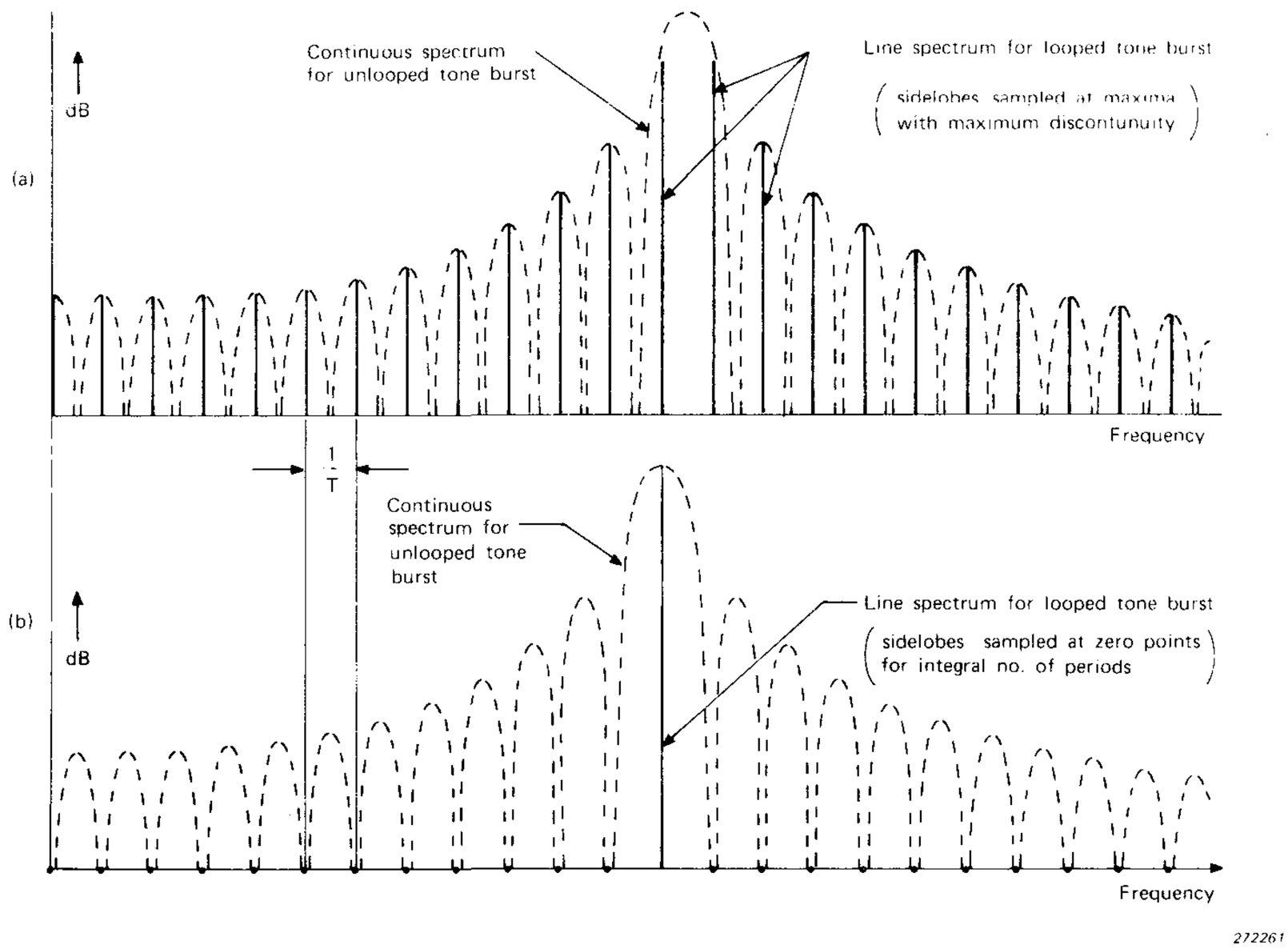

Fig.3. Line Spectra for Looped Tone Bursts obtained from corresponding Continuous spectra

In the following discussion, however, the continuous spectrum has been assumed, since this represents the worst case, and the fact that the spectrum is a line spectrum is neglected. It is shown later that the practical filter bandwidth should be greater than 1/T (which is equal to the Fourier line spacing) and this results in a continuous output spectrum again. It should be kept in mind that the periodicity was introduced artificially, and the output spectrum is to be compared with that obtained by direct analysis on the continuous signal.

Analysis with a Rectangular Window

It is desired to define conditions under which the results obtained from practical filters are either unchanged or only slightly modified in a well defined way by the effects of a rectangular time window. It is instructive to first examine the effects of analysis with an "ideal filter" and then investigate the modifications introduced by practical filters.

In Appendix A it is shown that the "overall filter characteristic" resulting from the convolution of an ideal filter shape with the spectrum of a rectangular time window generally has a bandwidth governed by the ideal filter, but a "skirt" governed by the window spectrum. This is also illustrated in Fig. 2c. For this reason, selectivity becomes the limiting property provided that the filter bandwidth is greater than the bandwidth of the window spectrum.

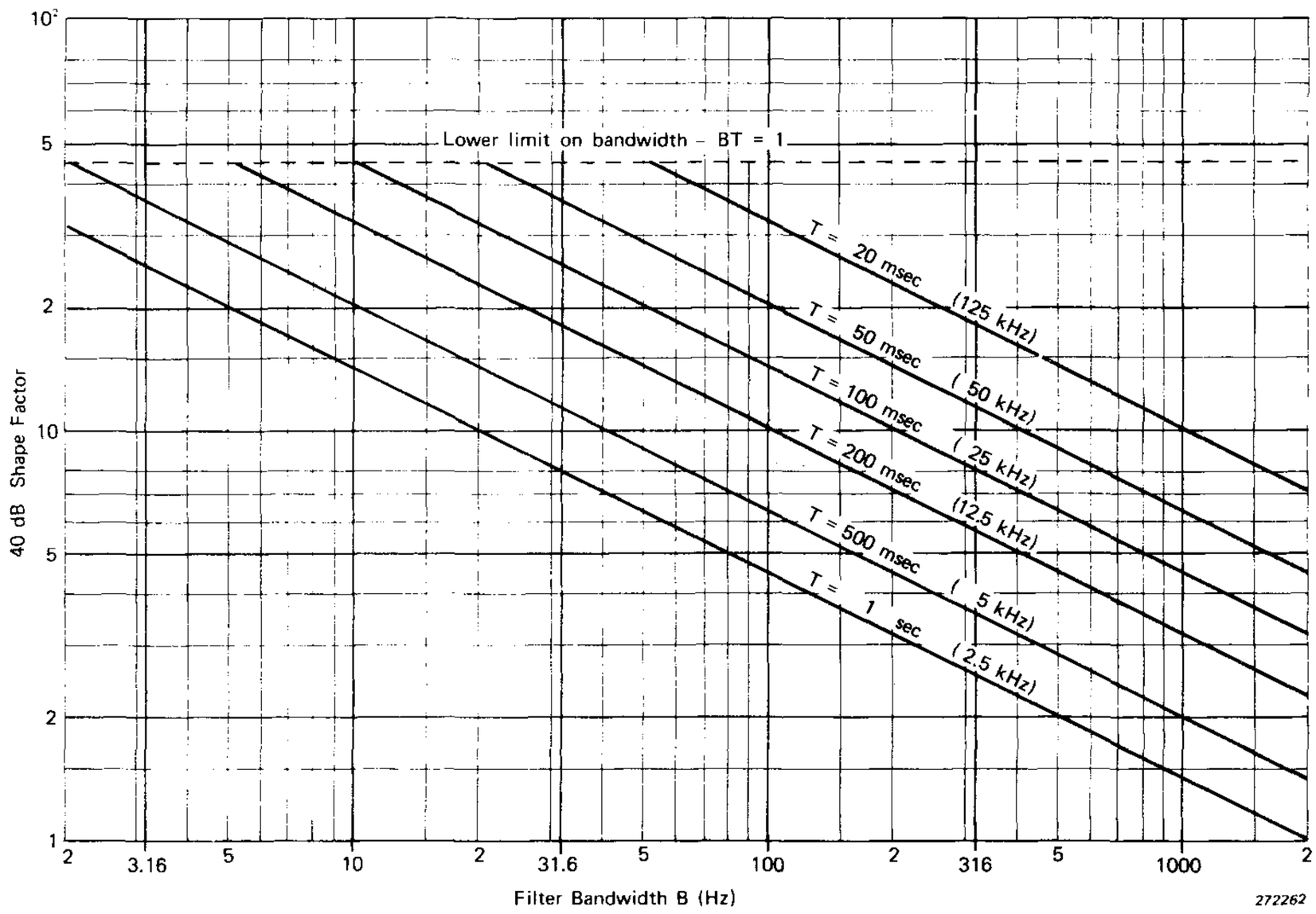

Fig. 4. 40 dB Shape Factor for Rectangular Window length T and Ideal Filter bandwidth B

For B & K filters, two systems are used to describe filter selectivity, viz. "Shape Factor", which is applicable to the heterodyne analyzers Types 2010, 2020 and 2021, and "Octave Selectivity", used in connection with the constant proportional bandwidth analyzers Types 2107, 2120 and 2121.

The standard definition of Shape Factor is the ratio of bandwidth of the filter characteristic at 60 dB attenuation to that at 3 dB attenuation. In the present context it is useful to define a "40 dB Shape Factor" (where the bandwidth at 40 dB attenuation is used instead) having regard to the dynamic range of the 7502 and the samll likelihood of having to separate closely spaced components differing by more than 40 dB. Fig.4 gives values of 40 dB shape factor against filter bandwidth and window length calculated as in Appendix A. Because of the relationship between window length and sampling rate with the 7502, this virtually puts a limit on the maximum frequency which can be analysed with a given bandwidth, in order not to exceed a given shape factor. These equivalent maximum frequencies are given in brackets in Fig.4 for a 7502 with 10K memory size, and should be reduced proportionally for smaller memory sizes. The graph also agrees with practical measurements made with the 2010 analyzer for 40 dB Shape Factor down to 4,5 (40 dB Shape Factor of the 2010 is 4). It is only rarely that the overall shape factor would be governed by the filter.

Octave Selectivity is defined as the attenuation of a filter one octave away from its tuned centre frequency, and is thus meaningful only for

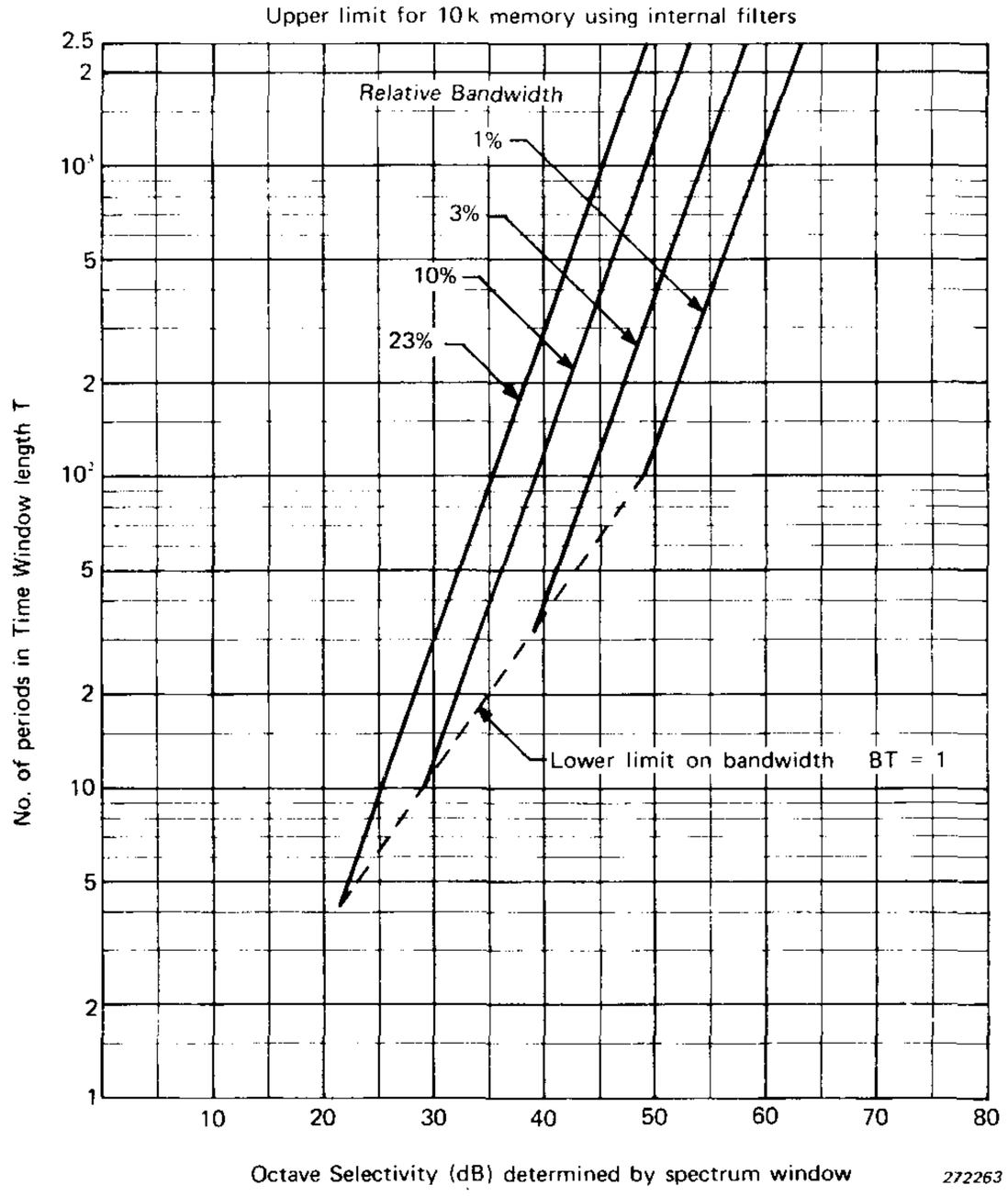

Fig.5. Octave Selectivity for Rectangular Window length T and constant percentage bandwidth Ideal Filters

constant proportional bandwidth filters. The definition assumed here is for fixed signal and moving filter, which results in the same value above and below the centre frequency. Fig.5 gives values of octave selectivity for the resultant "overall characteristic" against non-dimensional window length fT and relative bandwidth. This graph (for an ideal filter) has also been checked by practical measurements, with the 2120 analyzer, and found to agree well when the selectivity of the practical filter is somewhat superior to the values obtained from the graph, and for values of octave selectivity less than 50 dB (for values greater than 50 dB, the results are presumably affected by the dynamic range of the 7502). When the selectivity given by Fig.5 is of the same order as that of the analyzer, the results largely bear out the simple assumption that the contributions add by decibel addition. Thus, the amount by which the lower selectivity is to be reduced is given in Table 1 against the dB difference between them.

dB difference	0	2	6	10	⩾15
subtract from lower selectivity (dB)	3	2	1	0.5	0

Table 1. Decibel addition of selectivities

In this case, it is the lowest frequency which is limited by considerations of selectivity, the top frequency always corresponding to a quarter of the memory size when the inbuilt anti-aliasing filters of the 7502 are used (e.g. 2,5K periods for 10K memory size).

Note that it is customary to record the signal separately for analysis of each decade of the frequency range to be covered.

By frequency transformation to a playback rate of 100 KS/s, the analysis can then always be carried out in the highest decade permitted by the analyzers, viz. 2 kHz — 20 kHz corresponding to 200 — 2000 periods in a 10K memory. (The octave selectivity is thereby determined by the minimum number of periods viz. 200).

The dotted line on both figures 4 and 5 indicates the limit beyond which the filter bandwidth is less than the Fourier line spacing, and where the analysis bandwidth is no longer determined by the analyzer (see Appendix A). The separate spectral lines could also be confused with actual signal components. This requirement is expressed by

$$BT \geqslant 1 \qquad (1)$$

Analysis with a Gaussian Window

Many window shapes are an improvement on the rectangular, but the best appears to be the gaussian curve, since its Fourier transform is also of gaussian shape and thus not only has no sidelobes, but is very localised on the frequency scale. With a gaussian window it is shown in Appendix A that selectivity is no longer a limiting factor, but that the only limitation is given by effective analysis bandwidth. Defining the length T_G of the gaussian window as the length between the half amplitude points, it is shown that the minimum analyzer bandwidth B is defined by

$$BT_G \geqslant 2/3 \quad (\text{where} \quad T \geqslant 3\,T_G) \tag{2}$$

If B is made any smaller, the effective analysis bandwidth is no longer governed by it, but by the gaussian window spectrum.

Practical Analysis

Fig. 6 shows typical instrument setups, with which the high-speed analyses can be carried out, both with and without the Gauss Impulse Multiplier Type 5623.

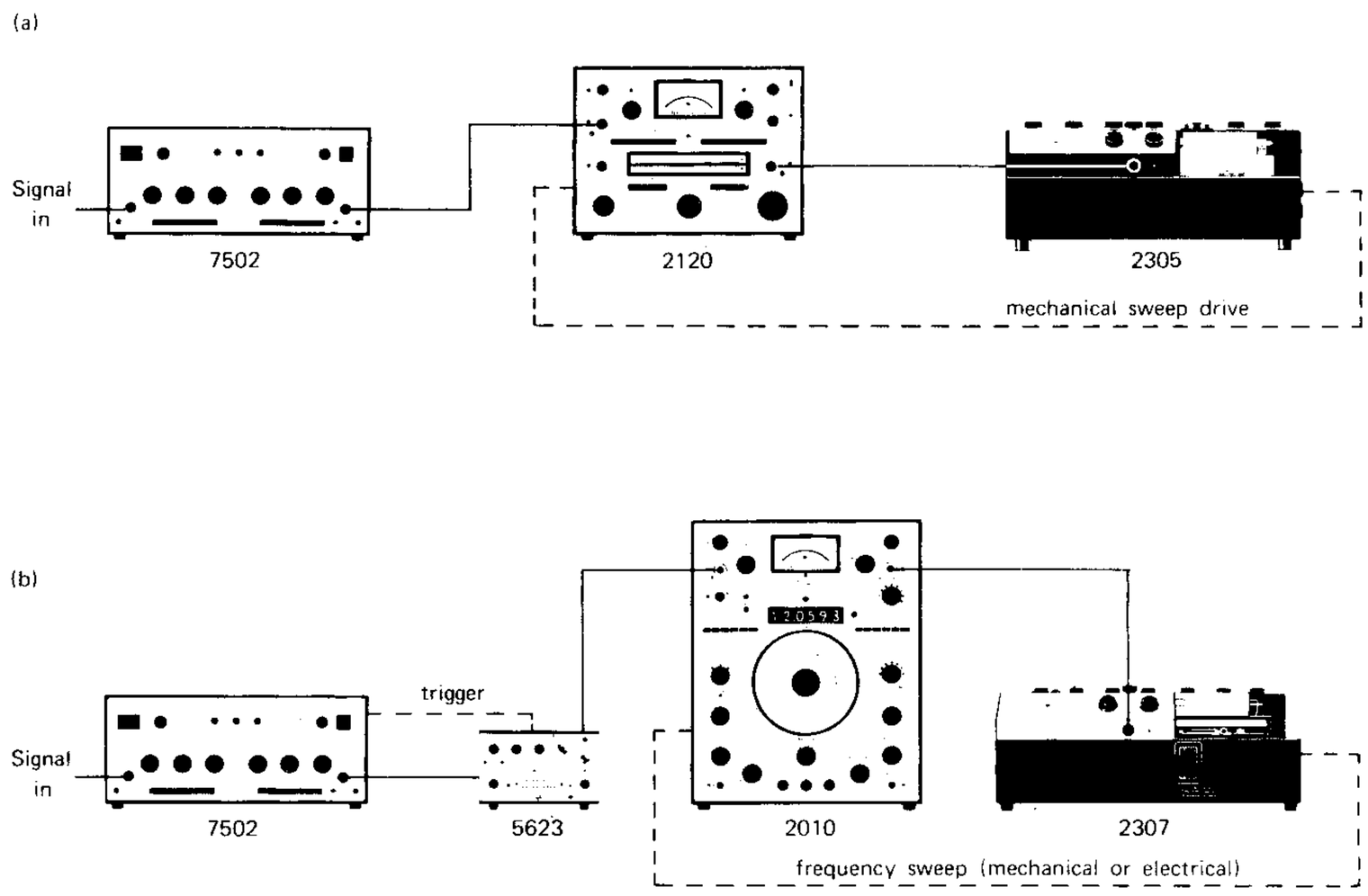

Fig. 6. Typical High-speed Analysis set-ups
(a) Without Gauss Impulse Multiplier
(b) With Gauss Impulse Multiplier Type 5623

The various factors involved are probably best illustrated in the following examples, which demonstrate typical savings in analysis time. Further details of the calculations are given in Appendix B.

Analysis speed has been determined in accordance with Ref. 3, of which the major results are summarized in Fig. 7.

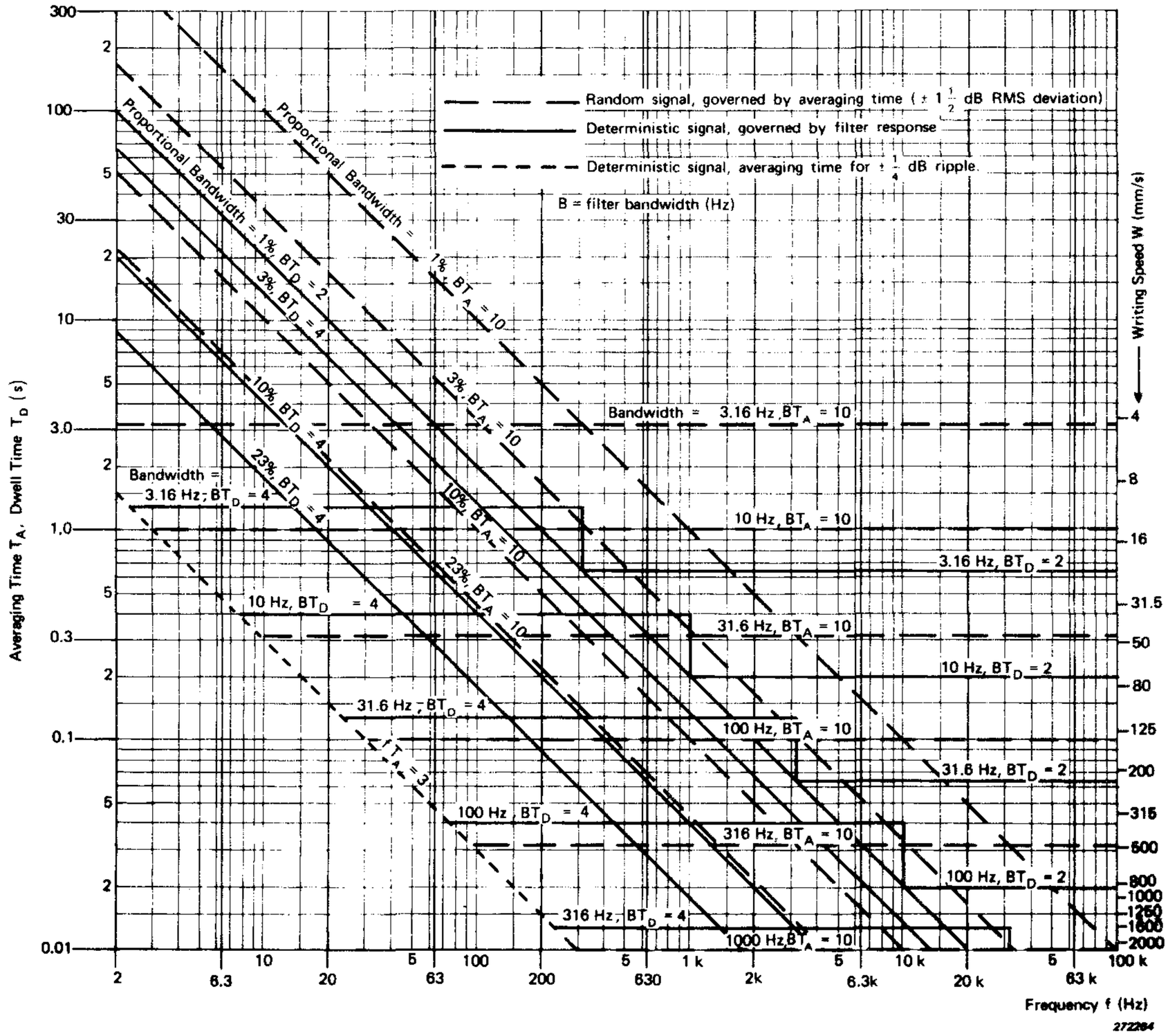

Fig. 7. SWEEP SPEED FOR SWEPT FREQUENCY ANALYSIS
For each bandwidth and frequency range, determine Filter Dwell Time, Averaging Time and Sweep Speed as follows:

1. Random Signal: *Dwell time T_D is always determined by averaging time T_A.*
From the graph read off T_D (= T_A) from the appropriate line for $BT_A = 10$ (horizontal lines for constant bandwidth, sloping lines for constant proportional bandwidth). This value will correspond to ± 1,5 dB RMS error. For a higher BT_A product and consequent reduced error, increase the value of T_A proportionally.
For DC recording *calculate sweep speed $S = B/T_D$.*

For AC recording, T_A is determined by recorder writing speed W and this can be read directly from the right-hand scale. Sweep speed can then be calculated from S = BW/100 (applicable to 50 dB potentiometer and 100 mm paper).

2. Deterministic Signal *(periodic or quasi-periodic): Read T_D based on filter response time from appropriate line for $BT_D = 4$ (or 2 where bandwidth ⩽ 1%). Read also minimum averaging time T_A based on ± 1/4 dB ripple from line $fT_A = 3$ (independent of bandwidth).*

For DC recording *calculate sweep speed based on filter response as $S = B/T_D$.*

For AC recording, *read off writing speed W corresponding to T_A and calculate sweep speed based on recorder response as S = BW/100. The governing sweep speed is the lesser of this and the value as calculated for DC recording.*

In all cases where sweep speed is governed by filter response time, increase T_A to the highest value which does not affect sweep speed.

Note (1) Averaging times will normally be constant over at least a half decade, whereas filter response times change automatically with frequency.

Note (2) S will be in Hz/s for B in Hz, but will be directly in mm/s for B expressed as equivalent recorder paper length in mm

Example (1): Constant Bandwidth Analysis (2010 Analyzer)

Given Data: Deterministic signal, frequency range 30 — 1000 Hz.
Analysis bandwidth 3,16 Hz.
Linear frequency scale and linear frequency sweep.

Such an analysis has been carried out, and the results are illustrated in Fig.8.

Fig.8(a) shows the results of a normal analysis which took 12 minutes, as can be determined from the information in Fig.7. Recording on the 7502 at 5 KS/s, (retaining frequencies up to 1250 Hz) it is possible to obtain a speed-up ratio of 100:1 by playing back at the maximum rate of 500 KS/s. The range for analysis is then transformed to 3 — 100 kHz, with equivalent bandwidth 316 Hz, both possible with the 2010 Analyzer. The minimum available averaging time of 0,1s is 5 times the memory cycle time of 20 ms, thus satisfactorily eliminating fluctuations (Ref. 3). The sweep speed is however limited by this averaging time and the resulting analysis (Fig.8(b)) is found to be only 10 times faster than

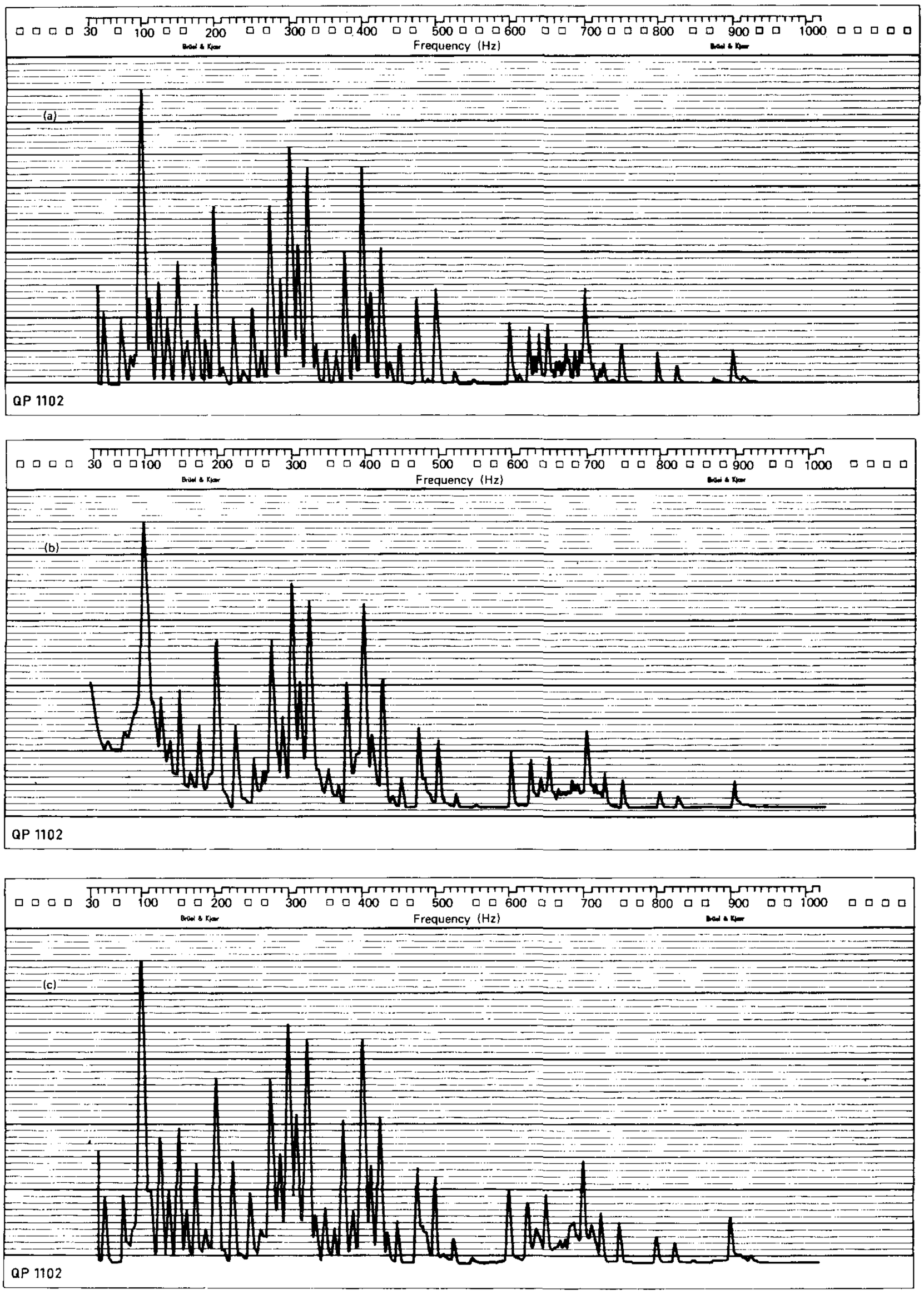

Fig.8. (a) Direct Analysis (See Example 1).
(b) High-speed Analysis using 7502 alone.
(c) High-speed Analysis using 7502 and 5623

the original (72 seconds). From Fig.4, the 40 dB shape factor is found to be 18, and the meaning of this can be seen by comparison of Figs.8(a)

and 8(b). The broadening of the base of the characteristic can clearly be seen, but the most important features of the analysis are still retained.

Fig. 8(c) shows the result of adding the Gauss Impulse Multiplier. This high-speed analysis has just as much detail as the direct analysis, Fig. 8(a).

The results can perhaps best be generalised as the time taken to analyze the frequency range 0 — 100 kHz with various bandwidths, assuming the maximum playback rate of 500 KS/s. This is given in the following table.

Bandwidth (Hz)	1000	316	100
Analysis Time (s)	25	74	245

Table 2. Constant bandwidth analysis time for the frequency range 0 — 100 kHz

Note that at max. playback rate and 10K memory size, 100 Hz is the smallest standard bandwidth which can be used with a rectangular window in order to satisfy Expression (1) ($BT \geqslant 1$), but this is in any case equivalent to a 1250 line spectrum.

Use of the Gauss Impulse Multiplier Type 5623 restricts in general the playback rate of the 7502 to 100 KS/s (upper limiting frequency 20 kHz) and slows down the analysis accordingly. On the other hand this can often be offset by the use of a smaller memory size, since a long record length is no longer necessary to obtain high selectivity. The reduction is of course limited by Expression (2).

Example (2): Constant Proportional Bandwidth (DC recording)
Given Data: Deterministic signal, frequency range 2 — 2000 Hz.
Analyzer Type 2120, bandwidth 3%
Recorder paper QP 1130

Here the normal analysis time determined from Fig. 7 is nearly 90 min. of which 70% is used for the lowest half decade. (For highest efficiency it is assumed that the averaging time is decreased and analysis speed increased by a factor of $\sqrt{10}$ for each half decade, but this of course requires operator supervision).

Although the analyzer in this case limits the analysis to 20 kHz maximum frequency, the total analysis time can still be reduced to less than 4 min. This is achieved by recording separately at rates of 0,1, 1 and 10 KS/s and by always playing back at 100 KS/s, analyzing in the decade from 2 — 20 kHz. Thus the first time, the decade 2 — 20 Hz is analyzed, the second time 20 — 200 Hz and so on. The standardisation of the analysis range considerably simplifies the analysis, as paper speed and averaging time (0,3s) are never altered. Between decades it is only necessary to switch the 7502 to the new recording rate, re-record, playback, switch the 2120 frequency range knob back two half decades and then start the level recorder. The level recorder can be operated in "single chart" mode (as this covers one decade on paper QP 1130) and thus synchronisation between level recorder and analyzer is never altered.

The results have been generalised in the following table (neglecting time spent between scale ranges etc.).

DC Recording (Type 2120)	Bandwidth	23%	10%	3%	1%
	Analysis time per decade (s)	22	22	74	220

Table 3. Constant proportional bandwidth analysis time per decade (DC recording)

Since the lowest frequency analyzed at any time corresponds to 200 periods in a 10K memory, the minimum octave selectivity from Fig.5 is 47 dB. Table 1 shows that this dominates over the octave selectivity of the analyzer itself (59 dB), so that the overall selectivity is also 47 dB.

If the Gauss Impulse Multiplier were used, the minimum standard value of T_G permitted by Expression (2) is 20 ms, but this would permit reduction of memory cycle time to 60 ms (6K memory size) which would allow retention of the same averaging time (0,3s) and thus the same analysis speed. The octave selectivity would then be dominated by the analyzer (59 dB).

Example (3): Constant Proportional Bandwidth (AC recording)
Given Data: Random signal, frequency range 20 Hz — 20 kHz.
Analyzer 2107, bandwidth 6%
Recorder paper QP 1130

The major difference in this case is caused by the necessity for AC recording. The averaging time is determined by the writing speed setting of the level recorder, and as shown in Ref. 3, the paper speed is limited by the writing speed rather than by the averaging time itself. The same applies to both normal analysis (of random signals) and the high speed analysis.

From Fig.7 it can be determined that the normal analysis time is over 45 min., and in fact to achieve a suitably high averaging time at the lowest frequency, the "Potentiometer Range dB" knob has to be set to 80 (Ref. 3).

For the high speed analysis, the three recording rates 1, 10 and 100 KS/s are used, while playback is again at 100 KS/s. In order to match the required averaging time of 0,3s (as for Ex. (2)), Fig.7 indicates a writing speed of 50 mm/s, but this can be increased to 80 mm/s if the "Potentiometer Range dB" knob is set to 80 (Ref. 3). The high speed analysis can then be carried out in under 4 min.

This illustrates that even for a signal in the normal audio frequency range, there is a considerable advantage to be gained from always analyzing in the highest decade (the lowest decade, which dominates the normal analysis time, is played back 100 times faster).

The octave selectivity from Fig.5 is 44 dB as compared with 45 dB for the 2107 analyzer itself. The resulting overall selectivity of 41,5 dB (Table 1) would rarely affect the results of analysis, in particular on a random signal, and thus the Gauss window would generally not be required with this analyzer.

Another point of interest is that the BT product determined by the record length has a lower value of 12, and this is a basic limitation, since it can only be increased by increasing percentage bandwidth.

If the Gauss Impulse Multiplier were used, then the minimum bandwidth would be even further restricted, since the effective record length is then reduced to 0,43 times the total impulse length (1,3 times the half amplitude length, using the calculation method given in Ref. 4.)

With AC recording, the analysis is slower by at least a factor of 3 as shown by the generalised figures in the following table.

AC Recording (Type 2121)	Bandwidth	23%	10%	3%	1%
	Analysis time per decade (s)	22	74	220	734

AC Recording (Type 2107)	Bandwidth	29%	21%	16%	12%	8,5%	6%
	Analysis time per decade (s)	22	22	74	74	74	74

Table 4. Constant proportional bandwidth analysis time per decade (AC recording)

Other Advantages

Other advantages apart from savings in analysis time are as follows:

1. Ability to achieve narrower effective bandwidth than that possible with a constant bandwidth analyzer, e.g. it may be desired to analyze some signals with a bandwidth less than the 3,16 Hz available on the 2010 analyzer.

2. Where tape recording is to be carried out in the field, for subsequent analysis in the laboratory, this recording need only be as long as the required data sample, rather than the total normal analysis time. This can give a considerable reduction in recording time, particularly on low frequency signals.

3. Ability to analyze short data records, e.g. short sections of a non-stationary signal.

4. Ability to transform low frequency signals up into the range of the analyzer.

Summary and Conclusions

It is possible using the Digital Event Recorder Type 7502 to speed up spectrum analysis by recording a signal at low frequency and playing it back at the top rate governed by either the 7502, the analyzer used, or the Gauss Impulse Multiplier Type 5623. A frequency range of analysis of one decade can suitably be covered with each recording.

If no special shaping function is used, the sudden transition at the signal junction point modifies the spectrum being analyzed (in the worst case) in the same way as a sweeping filter whose characteristic is the Fourier transform of the rectangular "time window" equivalent to the recorder memory length. In combination with the analyzer filter, the to-

tal effect is generally to broaden the base of the overall filter characteristic, thus reducing selectivity, without altering the effective bandwidth appreciably. There is a lower limit on analyzer filter bandwidth, however, below which the effective bandwidth is determined by the window function. Figs.4 and 5 indicate the effects on selectivity, for constant bandwidth and constant proportional bandwidth respectively, and also indicate the minimum valid bandwidths.

If the reduced selectivities cannot be accepted, use can be made of the Gauss Impulse Multiplier Type 5623 to produce a smoothly contoured window function which has a much less disturbing effect in the frequency domain. The minimum usable bandwidth is at least doubled, but for all larger bandwidths the selectivity will be governed by the analyzer. One other effect of the gaussian window is that the effective record length (with regard to accuracy of estimates on random signals) is reduced to a maximum of 0,43 times the memory cycle length. This restricts the analysis of random signals to a minimum bandwidth corresponding to approximately 1% of the highest frequency, as opposed to 0,5% with a rectangular window. For constant proportional bandwidth and assumung analysis over one decade at a time, this results in minimum bandwidths of 10% and 5% respectively, (see Example (3)). This is not expected to be a serious limitation however, since a highly selective characteristic is normally only required with deterministic signals. The use of the 5623 can result in slower analysis, however, for two reasons

(a) Its top frequency of 20 kHz limits the playback rate of the 7502 when analyzing with the 2010 Analyzer.

(b) The ratio of averaging time to record length may have to be increased to damp out fluctuations (Ref. 3) but this can often be offset by reducing record length. (See Example (2)).

It is perhaps worth mentioning that although the discussion has centred around the analysis of stationary signals, the instrument systems are also applicable to the analysis of non-stationary signals, particularly when the Gauss Impulse Multiplier is included. As examples could be taken the analysis of speech or bio-medical phenomena. If short sections of the signal in the 7502 memory were selected for analysis by means of the Tape Signal Gate Type 2972 (rectangular window) then Figs.4 and 5 can still be used to predict the overall filter characteristic (with T now equal to the window length rather than the memory cycle time). Since in that case it is not likely to be possible to include sufficient periods of the lowest frequency in the window length to give an

acceptable overall characteristic, it is much more likely that a gaussian window will be needed instead. Expression (2), is still valid, even when the gaussian window occupies a smaller fraction of the total memory length, but the frequency range over which analysis can be made is restricted accordingly. The method is probably most applicable to constant bandwidth analysis with a linear frequency scale, where the useful frequency range is limited to 1,5 decades or so. Attention would have to be paid to crest factor, where RMS detection is used for the analysis (as assumed elsewhere in this paper), but perhaps in some cases this problem could be overcome by using peak detection methods (Ref. 2).

References:

1. G. M. JENKINS and D. G. WATTS: "Spectral Analysis and its Applications", Holden — Day, San Francisco, 1968

2. JENS T. BROCH and H. P. OLESEN: "On the Frequency Analysis of Mechanical Shocks and Single Impulses", B & K Technical Review No. 3, 1970

3. R. B. RANDALL: "Analysis Time for Swept Frequency Analysis", B & K Application Note No. 13—054

4. JENS T. BROCH and C. G. WAHRMAN: "Effective Averaging Time of the Level Recorder Type 2305", B & K Technical Review No. 1, 1961

5. R. B. BLACKMAN and J. W. TUKEY: "The Measurement of Power Spectra", Dover, N.Y. 1959

6. A. A. KHARKEVICH: "Spectra and Analysis", translated from Russian, Consultants Bureau, New York, 1960

Appendix A

Filter Characteristics resulting from Time Windows

As discussed in the Main Section, the multiplication of a signal by a window function in the time domain results in a convolution of their respective Fourier spectra in the frequency domain.

Thus if $p(t) \rightarrow P(f)$

and $q(t) \rightarrow Q(f)$

then $p(t) \cdot q(t) \rightarrow P(f) * Q(f)$

where the arrow represents Fourier transformation and the star represents convolution according to the integral

$$P(f) * Q(f) = \int_{-\infty}^{+\infty} P(\theta) \cdot Q(f - \theta)\, d\theta$$

Thus for each value of f, the convolution function represents a sum of all the components in $P(\theta)$ weighted by the function $Q(-\theta)$ displaced by an amount f.

Since P and Q are in general complex, this summation will be a vector addition, and the result dependent on the phase relationships of the various components. For a random signal, however, where the various components of $P(\theta)$ have random phase, they will add according to their relative energy contents, and thus the final power spectrum will be the convolution of the two power spectra. (Ref. 5). For a deterministic signal (periodic or quasi-periodic), the Fourier spectrum consists of a series of delta functions with phase according to the time at which the signal sample is taken. For each component considered separately the power spectrum of the convolution would be obtained as the convolution of the window power spectrum with the delta function as illustrated in Fig.2. For most practical purposes, therefore, the correct peak values of the power spectrum will be obtained at the frequencies of the components

by convolution of the power spectra of signal and time window, though phase relationships could affect the values at notches between components. It is generally the peaks in which we are interested, however, and so once again the latter convolution will give an adequate representation of the true power spectrum.

Thus the overall effect on the true power spectrum $|P(f)|^2$ is the same as convolving it with $|Q(f)|^2$ which can be considered as sweeping over it a filter with the characteristic $|Q(f)|^2$.

1. Rectangular window length T seconds

Fig.9 shows the power spectrum of a sinusoidal signal of frequency "f_o" multiplied by a rectangular window of length T. This has the form of a $((\sin x)/x)^2$ function, centered at frequency f_o and with side lobe width 1/T. (As indicated in Fig.2 there is also another function centred at $-f_o$, but if f_o is sufficiently high, the interaction can be neglected).

If this function is swept by any filter, the resulting convolution represents the "overall filter characteristic" with which the original sine wave is being detected. For an ideal filter of bandwidth B, the convolution is relatively simple, viz. the integration of the function over B for each position of the ideal filter. Fig.9 illustrates the integration areas for two

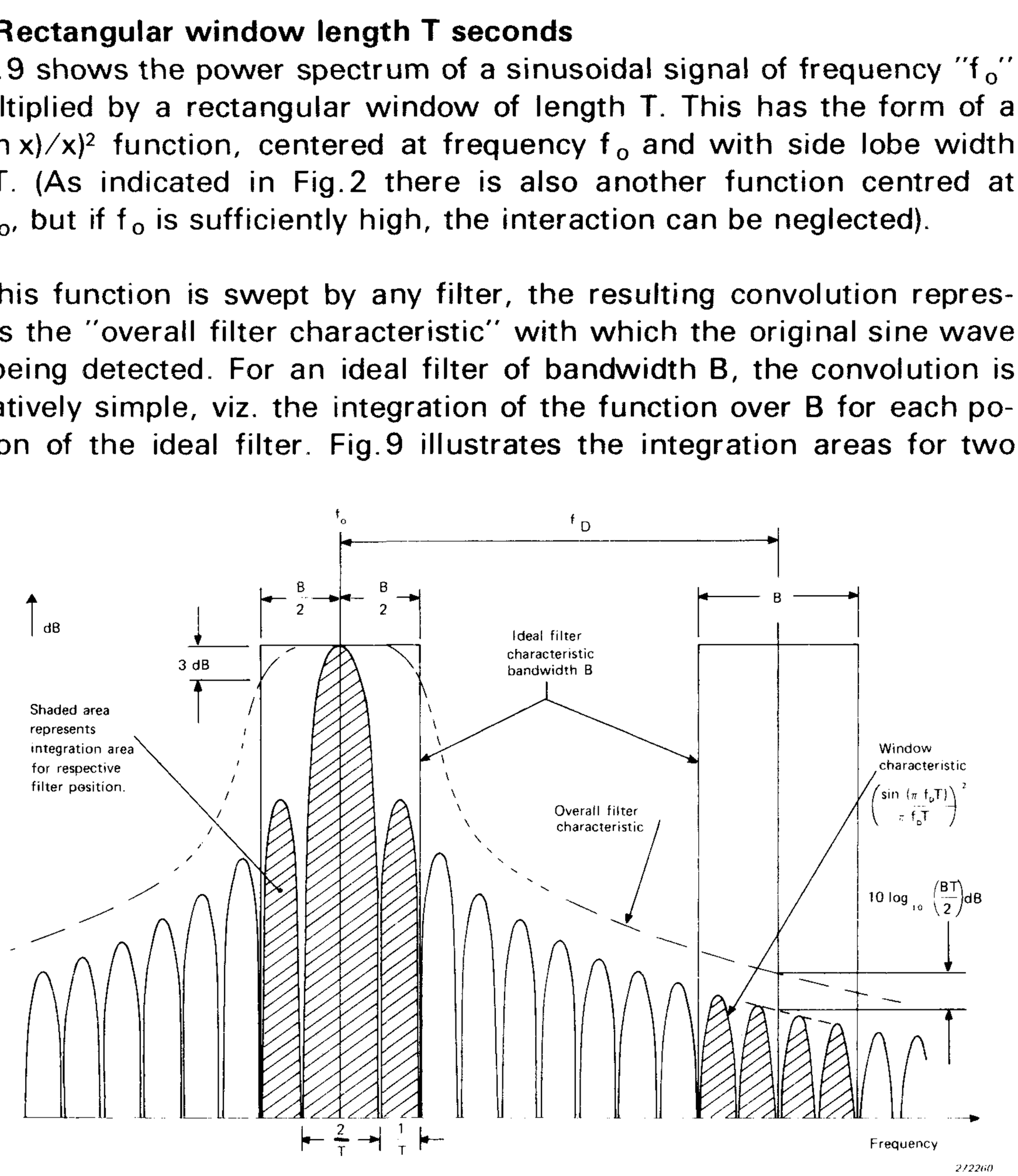

Fig.9. Determination of Overall Filter Characteristic for Rectangular Window and Ideal Filter

such positions. The main features of the characteristic can be determined by simple considerations. It can be seen, for example, that as long as the main lobe is contained within the ideal filter ($f_D < B/2 - 1/T$) there will be no appreciable attenuation. With one side of the ideal filter along the centreline of f_o ($f_D = B/2$) approximately half the total power will be transmitted and the attenuation will thus be close to 3 dB. Thus, the distance between the 3 dB points is B, indicating that the bandwidth is also B. Away from the passband ($f_D >> B/2 + 1/T$), if the ideal filter bandwidth equals the main lobe width ($B = 2/T$), it can be seen that since the main lobe and sidelobes have approximately the same shape, the convolution will have an attenuation approximately equal to that of the envelope of the $((\sin x)/x)^2$ function. For $B > 2/T$, the power transmitted by the ideal filter for $f_D >> B/2 + 1/T$ will be approximately proportional to its bandwidth, while that transmitted for $f_D = 0$ will be dominated by the main lobe and thus independent of the bandwidth. The net result is a reduction of attenuation equal to $10 \log_{10} N$ where $N (= BT/2)$ is the number of main lobe widths in the bandwidth B.

The overall attenuation is thus:

$$10 \log_{10} (x^2) - 10 \log_{10} \left(\frac{BT}{2}\right) = 10 \log_{10} \left(\frac{2 x^2}{BT}\right)$$

But from Ref. 2, $x = f_D \pi T$

where f_D = frequency displacement from sinewave frequency f_o.
T = time window length

resulting in the basic equation:

$$\text{attenuation} = 10 \log_{10} \frac{(2 f_D^2 \pi^2 T)}{B} \qquad \text{(A1)}$$

This formula has been checked by numerical*) calculation and found correct within 0,5 dB.

(1) Effective Bandwidth

This has also been checked numerically*) for the overall characteristic, based on the definition of effective bandwidth as the width of ideal filter which would transmit the same power from a white noise source. The following table gives values of effective bandwidth against BT (as defined in the previous section).

---

*) Trapezoidal integration was used for the numerical calculations, with step width = 1/5T.

BT	18	6	2	1,2	1	0,8	0
Effective	1.01 B	1.03 B	1.10 B	1.20 B	1.30 B	1.50 B	–
Bandwidth	18.2/T	6.18/T	2.20/T	1.44/T	1.30/T	1.20/T	1.00/T

Table 5. Effective Bandwidth for rectangular window

The value given for BT = 0 is the limiting case for an infinitely narrow filter. It can be seen that for BT down to 1, the effective bandwidth is governed by B and below that it is governed by lobe width 1/T. For BT = 1 the bandwidth is 30% greater than B.

(2) 40 dB Shape Factor

Using equation (A1) to calculate the frequency displacement f_D at which the skirt attenuation is 40 dB, and dividing by B/2 results in

$$\text{40 dB Shape Factor} = \frac{45}{\sqrt{BT}} \qquad \text{(A2)}$$

This formula is the basis of Fig. 4.

(3) Octave Selectivity

Let relative bandwidth = b

Then one octave above the tuned frequency f_o, $f_D = f_o$ and bandwidth B $= 2\,bf_o$

Substituting these quantities in Eqn. (A1) results in

$$\text{Octave Selectivity} = 10 \log_{10} \left(\frac{\pi^2 n}{b} \right) \qquad \text{(A3)}$$

where $n = f_o\,T$ = number of periods of frequency f_o in time window length T

Equation (A3) is the basis of Fig. 5, although the attenuation given there has been reduced by 1 dB to give a better fit to the experimentally measured points.

2. Gaussian Window, half amplitude length T_G seconds

The formula for this time window is:

$$e^{-\frac{t}{2\sigma^2}} \qquad \text{where} \qquad \sigma = \frac{T_G}{2{,}353}$$

The Fourier transform of this function (Ref. 6) is:

$$\sqrt{2\pi}\ \sigma e^{-2\pi^2\ f_D{}^2\ \sigma^2} = 1{,}072\ T_G\ e^{-3{,}56\ f_D{}^2\ T_G{}^2}$$

Since we are only interested in attenuation from the peak value, and absolute calibration will be carried out separately, this can be normalised to a peak value of unity as:

$$e^{-3{,}56\ f_D{}^2\ T_G{}^2}$$

The power spectrum window is the square of this function, which has an attenuation given by:

$$10\ \log_{10}\ [e^{7{,}12\ f_D{}^2\ T_G{}^2}] = 31\ f_D{}^2\ T_G{}^2\ \text{(dB)} \qquad \text{(A4)}$$

"Overall Filter Characteristic"

Because of the very different form of the spectrum window in this case, the filter characteristic from convolution with an ideal filter must be estimated differently. Fig.10 shows the spectrum window corresponding to equation (A4) on a dB amplitude scale, and also shows the areas over which integration is to be carried out for two positions of the ideal filter. These integrations can be determined from tables of the "Normal Probability Integral", or calculated numerically. Table 6 has been obtained by the latter means, and shows for various values of X (displacement from the centreline in terms of standard deviation σ), the area under the

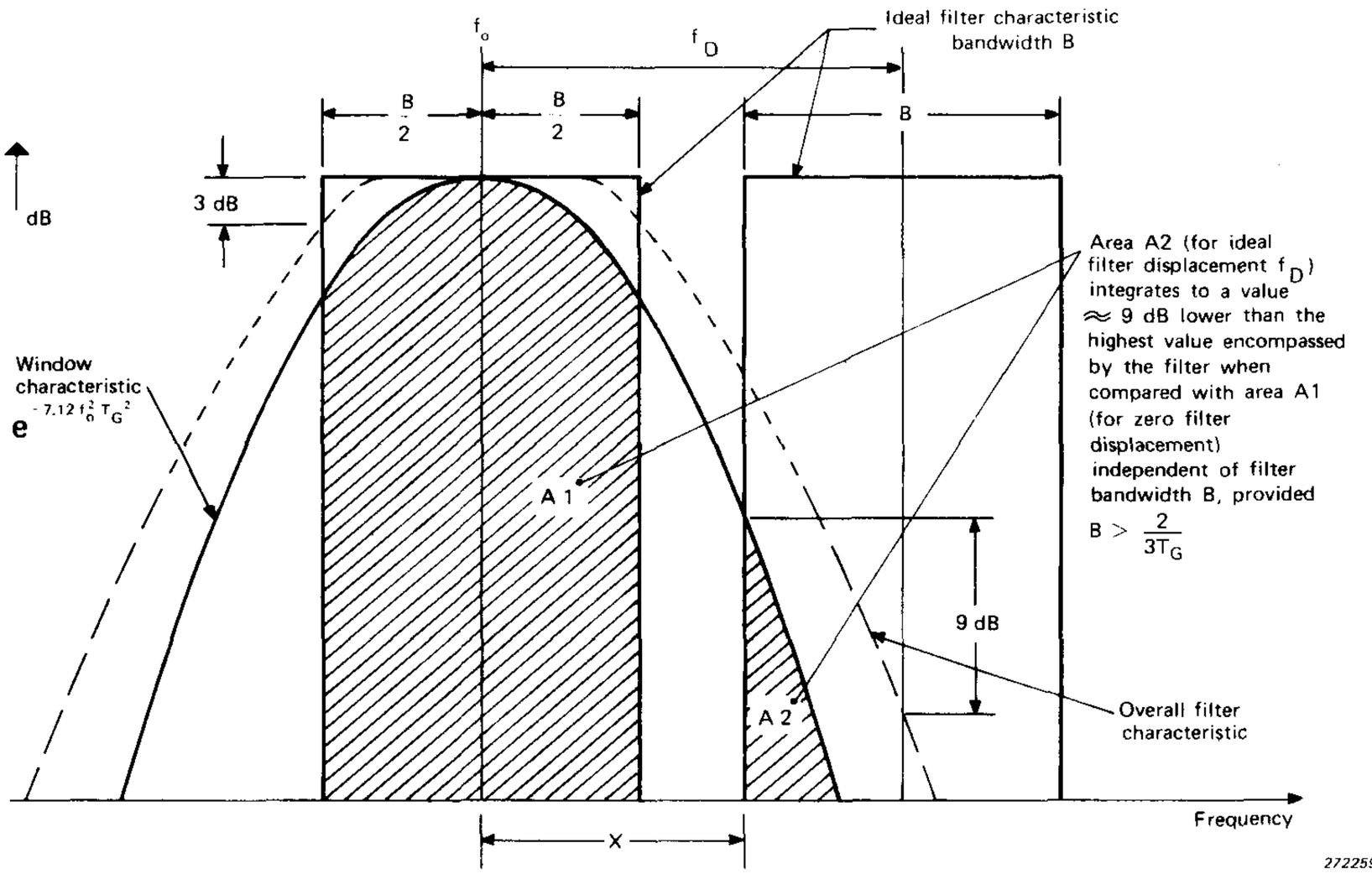

Fig.10. Determination of Overall Filter Characteristic for Gaussian Window and Ideal Filter

x	Area A2 for B→∞	Equivalent dB Attenuation	Attenuation of gaussian curve (dB)	Difference (dB)
2.33	10^{-2}	20.0	11.8	8.2
3.09	10^{-3}	30.0	20.7	9.3
3.72	10^{-4}	40.0	30.1	9.9
4.29	10^{-5}	50.0	39.5	10.5
4.75	10^{-6}	60.0	49.0	11.0
5.20	10^{-7}	70.0	58.7	11.3
5.61	10^{-8}	80.0	68.4	11.6

073021

Table 6. Properties of Gaussian Window characteristic (refer to Fig.10).

gaussian curve to the right of X (cf. area A2 in Fig.10) both as a proportion of the total area under the curve and also the decibel equivalent. This latter value represents the attenuation of the "overall filter characteristic", when the lower cutoff frequency of the ideal filter coincides with X, and where bandwidth B is large (B →∞). The attenuation of the gaussian curve itself at X is also shown (for the case where the curve represents power, or amplitude squared). From Table 5, it can be seen that for attenuations between about 20 and 50 dB, the difference between these two values is approximately 9 dB, and thus the value of the overall characteristic can be estimated as 9 dB lower than the highest value encompassed by the ideal filter. For larger attenuations this will be conservative. This relationship can be expressed in the form:

$$\text{Attenuation} \approx 31\,(f_D - \frac{B}{2})^2\ T_G{}^2 + 9\,\text{dB} \qquad \text{(A5)}$$

It can easily be checked that for most finite bandwidths there is only a negligible effect on this expression, and even for the minimum recommended bandwidth (see next section) this effect is only about 1 dB.

Effective Bandwidth

As for the case of a rectangular window, this has been checked numerically*), and the results are given in the following table:

---

*) Trapezoidal integration was used for the numerical calculations, with step width = $1/15\,T_G$

BT_G	6	2	.933	.667	.4	0
Effective	1.00 B	1.00 B	1.09 B	1.27 B	1.84 B	–
Bandwidth	$6.00/T_G$	$2.00/T_G$	$1.02/T_G$	$.848/T_G$	$.734/T_G$	$.664/T_G$

Table 7. Effective Bandwidth for gaussian window

These results demonstrate that $BT_G \cong 2/3$ is the lower limit beyond which the bandwidth is governed by the gaussian spectrum window.

40 dB Shape Factor
Using equation (A5)

$$40\,\text{dB}\quad \text{Shape Factor} = 1 + \frac{2}{BT_G} \qquad \text{(A6)}$$

This has a maximum value of 4, corresponding to the minimum value of $BT_G = 2/3$.

Since this is equal to the 40 dB shape factor of the 2010, selectivity will always be determined by the analyzer.

Octave Selectivity
In this case, from Eqn. (A5), it is found that

$$\text{Octave Selectivity} = 31\ (1 - b^2)\ n^2 + 9\ \text{dB} \qquad \text{(A7)}$$

$$\text{where}\quad n = f_o\ T_G$$

From this, the lowest value of octave selectivity obtainable (23% bandwidth, $BT_G = 2/3$) is 164 dB, so that once again the selectivity would always be determined by the analyzer.

Appendix B

EXAMPLE CALCULATIONS

Normal Analysis (See Fig.8)

(1) Deterministic signals — DC recording

Example No. & Frequency Range	T_D min (s)	T_A min	B equiv (mm)	$\frac{B}{T_D}$ (mm/s)	P (mm/s)	T_D actual	T_A actual	Analysis Time (s)
Ex. 1 30 – 1000 Hz	1.3	0.1	0.71	0.55	0.3	2.4	1.0	726
Ex. 2								
2 – 6.3 Hz	21	1.5	1.53	0.075	0.03	52.5	30	3667
6.3 – 20 Hz	6.6	0.5	1.53	0.24	0.1	17.5	10	1100
20 – 63 Hz	2.1	0.15	1.53	0.75	0.3	5.25	3	367
63 – 200 Hz	0.66	0.05	1.53	2.4	1.0	1.75	1	110
200 – 630 Hz	0.21	0.015	1.53	7.5	3.0	0.52	0.3	37
630 – 2000 Hz	0.066	0.005	1.53	24	10	0.17	0.1	11
								5292

(2) Random signal — AC recording

Example No. & Frequency Range	T_A min (s)	Equiv W (mm/s)	"Pot. range dB"	B equiv (mm)	$\frac{BW}{100}$ (mm/s)	$\frac{B}{T_D}$ (mm/s)	P (mm/s)	Analysis Time (s)
Ex. 3								
20 – 63 Hz	8.3	4*	80*	3.1	0.12	0.37	0.1	1100
63 – 200 Hz	2.6	4	50	3.1	0.12	1.2	0.1	1100
200 – 630 Hz	0.83	16	50	3.1	0.49	3.7	0.3	367
630 – 2kHz	0.26	50	50	3.1	1.5	12	1	110
2k – 6.3kHz	0.083	125	50	3.1	3.8	37	3	37
6.3k – 20kHz	0.026	500	50	3.1	15	120	10	11
								2725

* T_A = 5s

High Speed Analysis

(1) DC Recording

Example No. & Frequency Range	7502 Recording rate (KS/s)	7502 Playback rate (KS/s)	10k Record length T (s)	T_A (s)	B equiv (mm)	$\frac{B}{T_A}$ (mm/s)	P (mm/s)	Analysis Time (s)
Ex. 1 30 – 1000 Hz	5	500	0,02	0,1	0,71	7,1	3	73
Ex. 2								
2 – 20 Hz	0,1	100						37
20 – 200 Hz	1	100	0,1	0,3	1,53	5,1	3	37
200 – 2000 Hz	10	100						37
								111

(2) AC Recording

Example No. & Frequency Range	7502 Recording rate (KS/s)	7502 Playback rate (KS/s)	10k Record length T (s)	T_A (s)	W (mm/s)	"Pot Range dB"	B equiv (mm)
Ex. 3							
20 – 200 Hz	1	100					
200 – 2kHz	10	100	0,1	0,3	80	80	3,1
2k – 20kHz	100	100					

Example No. & Frequency Range	$\frac{BW}{100}$ (mm/s)	$\frac{B}{T_A}$ (mm/s)	P (mm/s)	Min No. periods n = fT	Rel. Bandwidth b	bn = BT	Analysis Time (s)
Ex. 3							
20 – 200 Hz							37
200 – 2kHz	2,5	10,3	3	200	0,06	12	37
2k – 20kHz							37
							111

Calibration Problems in Bone Vibration with reference to IEC R 373 and ANSI S3. 13—1972

by

Mogens Dahm

ABSTRACT

In this paper is discussed the general requirements of an artificial mastoid and the mechanical impedance of human mastoids compared to the demands laid down in the two documents IEC R 373 and ANSI S.3.13-1972. Suggested threshold values for audiometric bone conduction calibration in terms of equivalent acceleration and force are explained and the comparability of two commercially available artificial mastoids are given as well.

SOMMAIRE

Cet article discute les exigences générales concernant un mastoïde artificiel et l'impédance mécanique des mastoïdes humains en comparaison avec les exigences exprimées dans deux documents, CEI R 373 et ANSI S.3.13-1972. On explique les seuils suggérés pour l'étalonnage audiométrique par conduction osseuse en terme d'accélération et de force équivalents et on compare deux mastoïdes aritifciels disponibles sur le marché.

ZUSAMMENFASSUNG

Die allgemeinen Forderungen an ein künstliches Mastoid werden im Zusammenhang mit IEC R 373 und ANSI S.3.13-1972 besprochen und mit den natürlichen Gegebenheiten des menschlichen Mastoids verglichen. Zu den für die Knochenleitungs-Audiometrie vorgeschlagenen Schwellwerten, werden äquivalente Beschleunigungen und Kräfte angegeben, ferner Vergleichswerte für künstliche Mastoide zweier Fabrikate.

Introduction

In bone conduction threshold measurements it is essential to have calibrated measurements in order to obtain repeatable results. This is achieved by using a mechanical coupler, which provides a mechanical load impedance equal to that of the average human forehead or mastoid.

By transferring a bone vibrator to an artificial mastoid, previously calibrated in terms of output voltage for a given acceleration or force applied to its surface, it is possible to express the human threshold as an equivalent acceleration or force on the artificial mastoid. In this form the threshold data can be readily applied to the calibration of audiometers in everyday use. Furthermore, objective comparisons are facilitated between data obtained in different laboratories.

The requirements for an artificial mastoid can be summarized as follows:

1. The bone vibrator under test must be presented to the same mechanical impedance as the average human mastoid over the required frequency range which is usually from 250 Hz to 4000 Hz.

2. When the bone vibrator is pressed against the artificial mastoid in the same manner as when fixed to the human mastoid the motion of the bone vibrator should be indicated in terms of vibration amplitude, velocity, acceleration or force by means of a built-in vibration transducer.

3. The elements of the artificial mastoid should be stable with time.

The mechanical impedance of the artificial mastoid should depend on static force of application, frequency, and contact area of the bone vibrator in the same way as that of the human mastoid.

Standards concerning bone vibrator calibration

Both the IEC Recommendation R 373 and the American National Standard ANSI S3.13-1972 specify identical mechanical impedance characteristics of an artificial mastoid for the calibration of bone vibrators used in audiometry, see Table 1. The artificial mastoid is intended for use with bone vibrators having a plane, circular contact lip area of 1,75 cm^2, applied with a static force of 5,4 N covering the frequency range of measurement from 250 Hz to 4000 Hz. The IEC Recommendation also agrees with a related ISO draft Recommendation.

The above mentioned impedance values have been derived from earlier measurements (Ref. 4). With the development of more suitable impedance transducers*) having a low internal mass and use of automatic equipment, it has now been possible to compare impedance measurements on human beings faster and more accurately.

---

*) Brüel & Kjær Impedance Head Type 8000

Frequency Hz	Mechanical reactance Nsm^{-1}	Mechanical resistance Nsm^{-1}
250	−140	36
315	−110	29
400	− 89	25
500	−71	22
630	−55	20
800	−42	19
1000	−32	18
1250	−23	17
1500	−17	17
1600	−15	17
2000	−8.4	17
2500	−2.2	18
3000	2.7	18
3150	3.9	18
4000	10	19

Table 1. Mechanical impedance components for an artificial mastoid as specified in IEC R373 and ANSI S3.13-1972

Comparing the mechanical impedance of human mastoids at a static load of 5,4 N to the IEC R373 and the ANSI S3.13-1972 in Figure 1, the following characteristics are evident:

1. The human mastoid in general is softer (has a lower impedance) than that described in the standards.

2. The standard impedance curve as a function of frequency has a smooth run and does not show the typical pronounced dip around the resonance of the corresponding single impedance curves measured on human heads. The resonance is between 1500 Hz and 3000 Hz, depending on the person's skin thickness. This resonance is in general a simple resonance, where only the three parameters mass, stiffness and damping are the defining elements. At lower frequencies these parameters change, in particular the damping is heavily dependent on frequency.

The standard impedance curve is averaged from impedance values measured on a large number of persons, which explains the flatter response indicated in the standards. As resonant frequencies for different persons are spread over a complete octave an averaging will make the curve flatter with no pronounced resonance. For human mastoids there is a considerable variation in mechanical impedance for different static loads and it is desirable to retain this effect in an artificial mastoid. This is made by the viscoelastic impedance determining elements of the Arti-

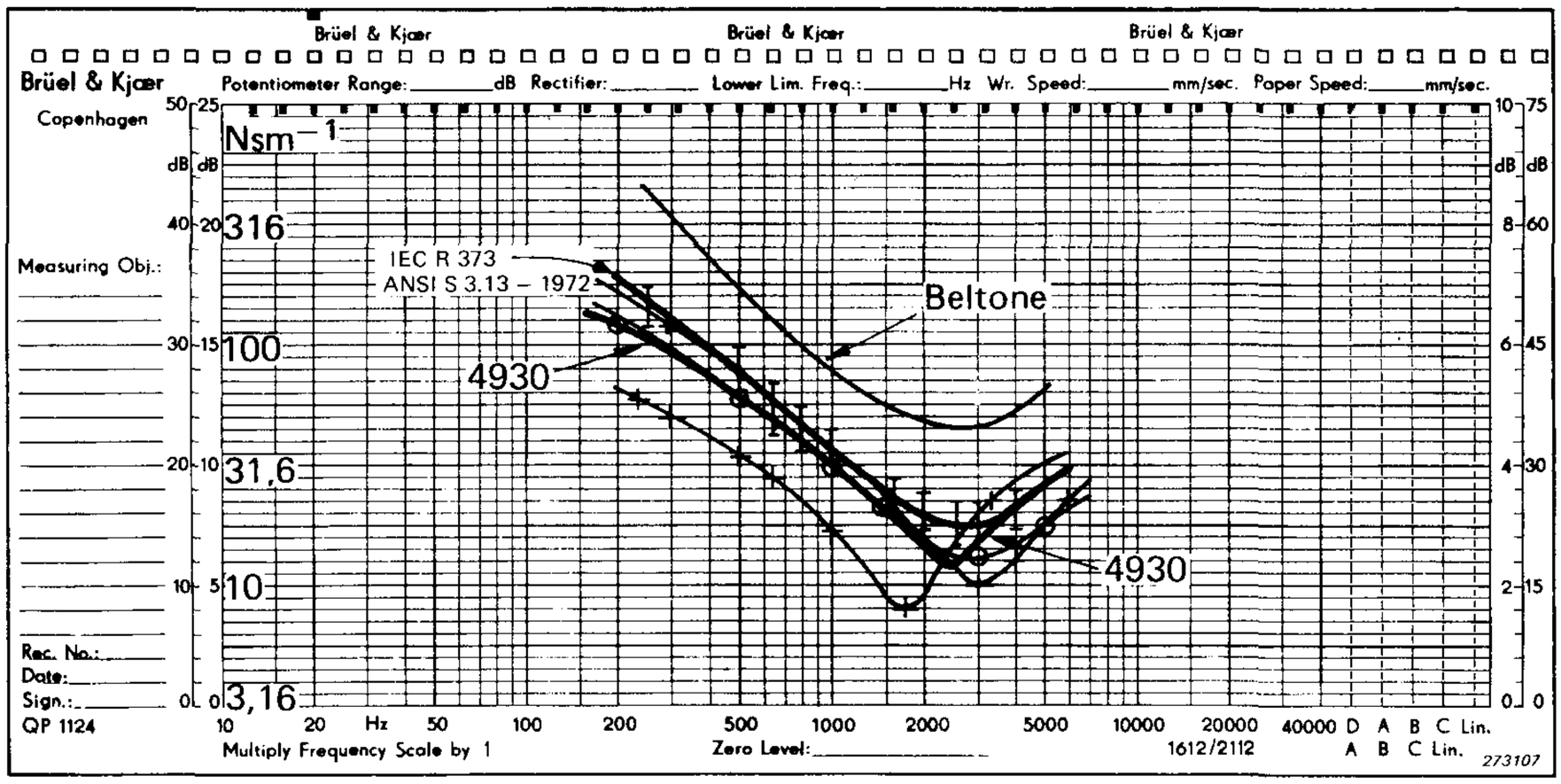

Fig. 1. Comparison of mechanical impedance.
IEC R 373 and ANSI S3.13-1972 with tolerances
o-o-o Average of 49 human mastoids (measured by Diestel and Brinkmann, Germany).
+-+-+ Typical single human mastoids (measured at Brüel & Kjær)
Artificial Mastoid Type 4930 and Beltone Model 5A

ficial Mastoid Type 4930, which conforms with British Standard BS 4009:1966 as well as with IEC R 373. The artificial mastoid is also in accordance with ANSI S3.13-1972 within the required tolerances at most frequencies.

Reference bone conduction threshold

There is, as yet, no international agreement on a standard for the threshold of hearing by bone conduction. In the mid-sixties the National Physical Laboratory in England, organised a ring comparison of bone conduction threshold measurements on normal listeners as a contribution to the work of ISO/TC 43, the international committee studying the problem. Results were reported by laboratories in USA, France, Great Britain and Germany (Ref. 5).

The ultimate aim of the intercomparison was expression of the threshold data in terms of response of an artificial mastoid, which conforms to BS 4009:1966. The artificial mastoid calibration is known in volts per unit acceleration, and the threshold data are accordingly expressed as equivalent threshold acceleration.

Further investigations of the bone conduction threshold have recently taken place at the Institute of Audiology, University of Oslo, Norway (Ref. 6). The data obtained here are in agreement with the earlier international ring comparison tests, and until reference threshold values for bone conduction are established by ISO/TC 43, the following data listed in Table 2 are suggested by the Institute as reference threshold values.

The threshold values refer to a bone vibrator placed on the Processus Mastoideus and are given as equivalent threshold values for an artificial mastoid conforming with IEC R 373, e.g. the Artificial Mastoid Type 4930.

Frequency Hz	Threshold acceleration dB re 1 cm/sec^2
250	6
500	10
750	9
1000	7
1500	5
2000	10
3000	12
4000	14
6000	10

Table 2. Reference bone conduction threshold values (Ref. 6)

Comparison of measurements with different artificial mastoids

In the early sixties and independently of the work of the international ring comparison the Hearing Aid Industry Conference (HAIC) in the USA organised a programme of experiments to determine bone conduction thresholds. During the past years several more studies of bone conduction threshold on young adults with normal hearing have been obtained (Ref. 7).

The appendix of the ANSI S3.13-1972 lists the HAIC interim hearing threshold values for bone conduction, which are based on the use of a Beltone 5A artificial mastoid. Since the Beltone mastoid does not have the same mechanical impedance values as the Brüel & Kjær Artificial Mastoid Type 4930, another set of data must be used when checking calibration of audiometer bone vibrators with the 4930. Comparison measurements were recently made between the two different artificial mastoids (Ref. 8) and average values of these comparisons are given in Table 3 to provide numbers which may be related to those in the ANSI appendix when using the Artificial Mastoid Type 4930.

The threshold values are given as equivalent force in dB re 1 μ Newton at the vibrator surface for mastoid position. It is recommended that the data shown in Table 3 are used when the force calibration of a bone conduction system of an audiometer is checked with an Artificial Mastoid Type 4930 and when the values should refer to the HAIC interim data. The Artificial Mastoid Type 4930 yields lower indicated force levels than the Beltone unit for the same electrical input voltage to the bone vibrator. The difference may be added to the values given in the appendix of the ANSI standard as shown in Table 3.

Frequency Hz	Average difference between Beltone 5A and Artificial Mastoid Type 4930 dB	ANSI interim bone conduction threshold values. dB re. 0,1 dyne	Recommended force levels for mastoid thresholds when using Artificial Mastoid Type 4930. dB re. 0,1 dyne
250	1.6	63.0	61.4
500	6.8	57.5	50.7
750	9.7	49.0	39.3
1000	6.1	43.0	36.9
1500	5.1	40.5	35.4
2000	11.9	40.0	28.1
3000	3.9	30.5	26.6
4000	3.8	35.0	31.2

Table 3. Recommended values for relating Beltone 5A and Brüel & Kjær Artificial Mastoid Type 4930 (Ref. 8)

Conclusion

The publications IEC R373 and the ANSI S.3.13-1972 form a standardised basis for bone conduction measurements on artificial mastoids. Bone conduction threshold calibrations can now be determined using an artificial mastoid, e.g. Type 4930 with available bone vibrators. At present there exists international agreement on the mechanical impedance values, corresponding only to a static force of application of 5,4 N and a plane area of contact of 1,75 cm^2. Efforts are made to specify the bone vibrator tip size and shape, as well as the static force of application for which the standardised mechanical impedance characteristics apply.

Interim threshold values in terms of equivalent acceleration and force are used for bone conduction calibrations. However, further work should be encouraged in order to allow more progress in the international standardization as there is an increasing need for standardized bone conduction threshold values.

References:

1. BS 4009: 1966: An artificial mastoid for the calibration of bone vibrators, British Standards Institution 1966.

2. IEC RECOMMENDATION 373: An IEC mechanical coupler for the calibration of bone vibrators having a specified contact area and being applied with a specified static force. 1971.

3. ANSI S3.13-1972: American National Standard for an artificial headbone for the calibration of audiometer bone vibrators. American National Standards Institute, Inc. 1972.

4. CORLISS, E. L. R. and KOIDAN, W.: J. Acoust. Soc. Amer. 27, 1164-1172, 1955.

5. ROBINSON, D. W. and WHITTLE, L. S.: 2nd report on standardisation of the bone conduction threshold. National Physical Laboratory, Teddington, England. 1967.

6. FLOTTORP, GORDON: Bone conduction threshold data. Institute of Audiology, University of Oslo, Norway. 1972.

7. DIRKS, DONALD D. et al.: Toward the specification of normal bone-conduction threshold. J. Acoust. Soc. Amer. 43, 6, 1237-1242, 1968.

8. WILBER, LAURA ANN: Comparability of two commercially available artificial mastoids. J. Acoust. Soc. Amer., 52, 4 (2), 1265-1266, 1972.

Appendix

Threshold Calibration of Bone Vibrators

When referring to the threshold acceleration data given in Table 2, the acceleration sensitivity of the Artificial Mastoid Type 4930 should be used together with its frequency response curve at constant acceleration. The electrical output from an Artificial Mastoid Type 4930 equivalent to the acceleration threshold can be found at each frequency by comparing the threshold data from Table 2 with the acceleration sensitivity and the frequency response curve at constant acceleration given on the calibration chart, see Figure 2.

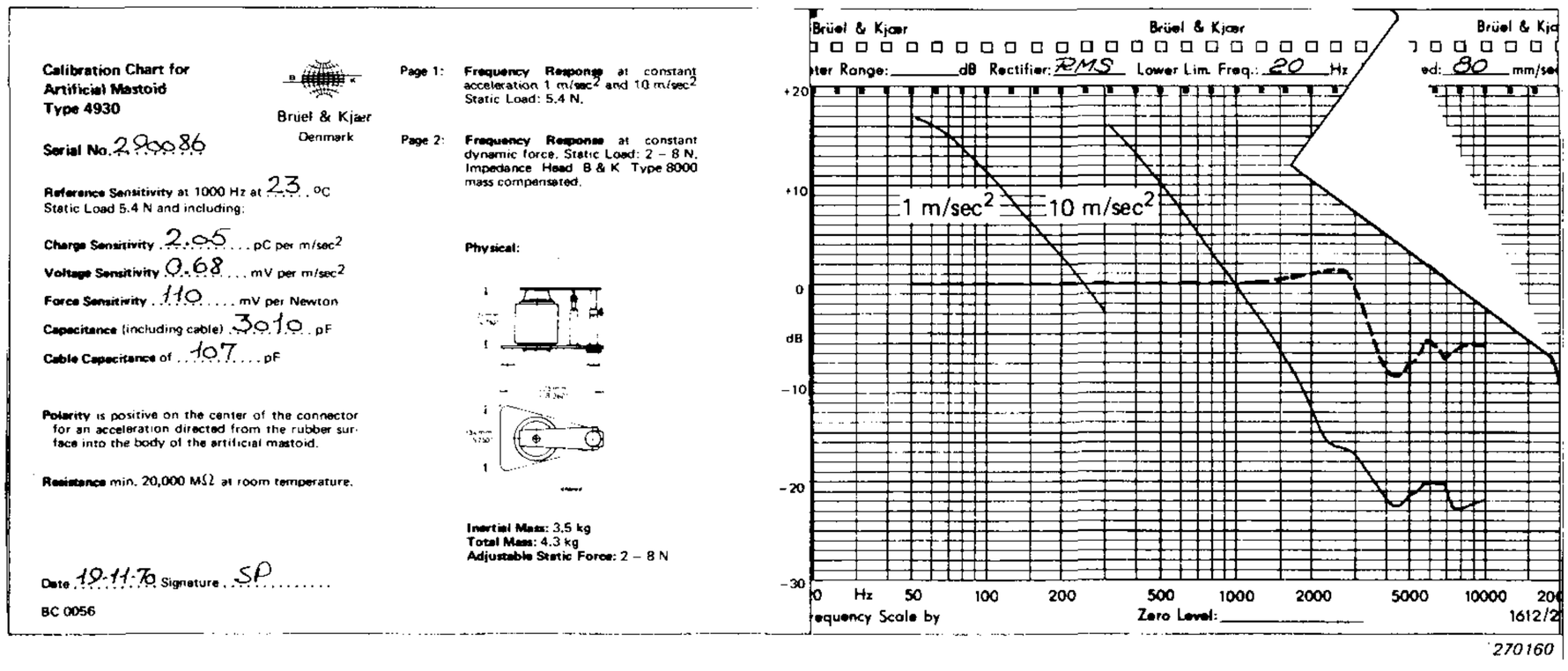

Fig. 2. Individual calibration chart for an Artificial Mastoid Type 4930

The acceleration reference sensitivity is stated in mV and pC per m/s^2 at 1000 Hz at a static load of 5,4 N. From the frequency response curve a sensitivity correction in dB is easily found for each frequency. By subtraction of 40 dB the sensitivity is obtained in mV or pC per cm/s^2 and, finally, addition of the appropriate data in dB from Table 2 yields the electrical output from the mastoid equivalent to the bone conduction threshold.

An Investigation of the Near-Field Screen Efficiency for Noise Attenuation

by

J. Stryjenski), D. Courtillat, E. Dubouloz, M. Lançon and J. Matusewics*

ABSTRACT

The paper describes model experiments which were carried out to check the performance of a noise reducing screen at the limit of its geometrical shadow. The measurements included a series of preliminary experiments to check the measuring set-up and the measuring room and to determine the relative distances source-screen-receiver for which diffraction laws are valid. Finally measurements were carried out to determine the influence of the screen length. The paper concludes that the screen efficiency at the geometric shadow limit conforms with that of optics theory whereby the noise reduction is equivalent to the effect of doubling the distance.

SOMMAIRE

L'article décrit des expériences sur modèles effectuées pour vérifier les performances d'un écran utilise comme protection contre le bruit dans le plan limité par l'ombre géométrique. Les mesures ont comporté une série d'expériences préliminaires destinées à vérifier le montage de mesure et la salle d'expérimentation. If s'agissait aussi de détermines les distances relatives source-écran-récepteur pour lesquelles les bois de la diffraction sont valables. Finalement, on a effectué des mesures pour étudier l'influence de la longueur de l'écran. La conclusion de l'article est que l'efficecité d'un écran à la limite de l'ombre géométrique est conforme aux résultats de la théorie optique disant que l'atténuation équivant à un doublement de distance.

ZUSAMMENFASSUNG

Zweck der hier beschriebenen Modellversuche ist, die Lärmminderung in der Randzone des geometrischen Schattens eines Schallschirms zu bestimmen. Es wird zunächst die Meßanordnung und der Meßraum untersucht, ferner diejenigen relativen Abstände zwischen Quelle, Schirm und Meßempfänger, für die die Beugungsgesetze gelten. Anschließend wird der Einfluß der Schirmlänge bestimmt. Nach den Ergebnissen gelten für die Randzone des geometischen Schattens die optischen Gesetze, demzufolge hat der Schirm die Wirkung einer Abstandsverdopplung.

---

*) Ecole d'architecture, Université de Genève

Introduction

Acoustical screens are one of the means used for isolation of noise in the open air. They may be either walls around patches of land, or light panels around working sites, embankments along roads, etc..

The screen efficiency depends upon the air-tightness and sound insulation capacity of the material as well as the geometric shape of the screen and its position relative to the sound source and the observer.

Airborne sound insulation is nowadays a well known problem. Most materials have a much higher efficiency when they are used for closed, air-tight partitions than when they are used for screens, which may be considered as limited, non closed partitions.

It is therefore necessary to know the acoustical phenomena related to the shape and the location of screens in order to be able to forecast their efficiency. It is then possible to optimize their size and location with respect to cost and although a 20 kg/m^2 air-tight partition gives an attenuation of approx. 24 dB, very rarely are the screens of a comparable efficiency.

Screen calculation methods have been taken from ondulatory optics which accounts for diffraction effects. The effect of diffraction on the edge of a screen is that light is partly radiated into the geometric shadow, thus reducing the screen efficiency.

Since similar phenomena occur in acoustics, it was thought that the optics results could be used to calculate screen efficiency. However, geometrical conditions leading to the results are very different in optics and acoustics.

As the scale to which any ondulatory phenomenon is referred is wavelength, it may be of interest to compare optical and acoustical conditions for any source-observer system. The relationship between wavelength, frequency and velocity is, in optics as well as in acoustics:

$$\lambda \cdot f = c$$

where λ = wavelength (m)

f = frequency (Hz)

c = velocity (m/s)

Red light wavelength is approx. 75×10^{-8} m, and is the longest wavelength in visible light. In the audio frequency range, the longest wavelength is approx. 20 m, and wavelengths concerned with noise reduction are in the range of 3,5 m to 0,1 m, which corresponds to frequencies between 100 and 3400 Hz approximately.

A simple optics experiment is, for example, observation of the shadow projected by a screen on a plane placed at 25 cm from the screen the light source being at 1 m from the screen. To perform a similar experiment in acoustics, distances would need to be multiplied by the ratio of the acoustical to optical wavelength, i.e. the shadow would be observed 32,5 km from the screen while the sound source would be placed 130 km from the screen, in the best case (0,1 m wavelength). This, obviously is of no interest for town-planners as in most cases, the observer is only some tens of wavelengths from the screen, which means he is still very close to it. He is, therefore, in the close field whereas optical observation are made at millions of wavelengths from the screen (i.e. in the remote field). For this fundamental reason, approximations made for derivation of optics results cannot be accepted without verification. On the other hand the mathematical theory would become very complicated, even in the most simple cases, without approximations.

As simple models are almost never encountered when designing acoustical screens, only experiments carried out on special models developed would provide results that can be used for town-planning. The purpose of this study is to develop a system and a measuring method applicable on models of constructions in engineering and architecture, these constructions being planned for protection against transport noise. Since diffraction is closely related to wavelength, the wavelength must be reduced linearly to the scale of the model. [3].

Components of maximum noise perceived at a certain distance from the road are found to be in the frequency range 100 to 500 Hz, the corresponding wavelength being in the range 3 to 0,7 m [4,5].

Frequencies and wavelengths used for the experiments are given in Table 1.

In order to experimentally determine the domains where optical laws can be applied to acoustical models in the near-field, it was decided to

f (kHz)	6,3	8	10	12,5	16	20	25	31,5	40
cm	5,4	4,25	3,40	2,72	2,12	1,70	1,36	1,08	0,85

Table 1. Frequencies and wavelengths used for the experiments

take a series of measurements on a half-plane screen (y-z) limited by a straight edge (y) perpendicular to the x axis. Measurements are taken in the plane defined by the line between the source and the transducer and by the screen edge. Fig. 1 shows the corresponding configuration.

A B & K Noise Generator modified to extend in the range 31,5 — 50 kHz, was used as the noise source. A 1/2 inch Condenser Microphone was used to transmit filtered noise in octave bands. (Some experiments have however, been checked using a 4 cm loudspeaker). The noise was measured in 1/3 octave bands utilizing a 1/2" or 1" microphone and a B & K Spectrometer. Since airborne sound isolation across the materials used for the screen was always much greater than the shadow effect, transmission through the screen was neglected.

The experiments were divided into three groups.

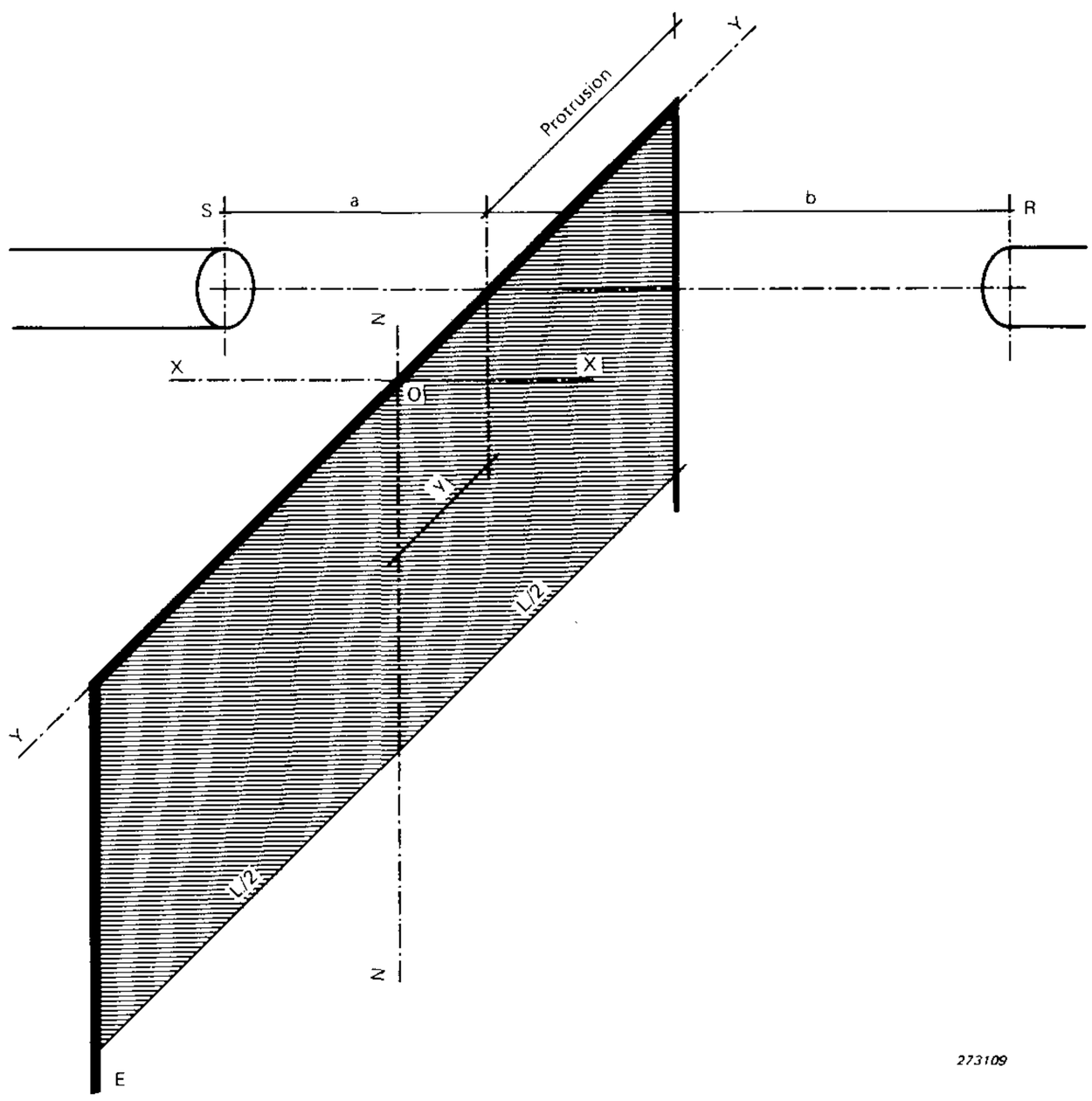

Fig. 1. The measuring set-up. S = source, E = screen, R = Receiver (mircophone) L = screen total length, a = source-screen distance, b = microphone-screen distance

Preliminary experiments for checking the measuring set-up and determining any disturbance of the sound field due to reverberation in the room and the presence of the screen.

Measurements in the near-field using a half-infinite plane in order to find the source-screen and screen-receiver distances for which diffraction laws are valid (16 experiments with 9 1/3 octave bands for each).

Measurements to find out for which length a screen can be considered as infinite (27 experiments, each in 9 1/3 octave bands)

It should be remembered that all experiments for the last two cases are made in the plane limiting the geometric shadow, i.e. in the x-y plane in Fig. 1.

Preliminary experiments

Reverberation

Although the test room of volume 40 m^3 was made highly acoustically absorbant, residual reverberation could have given raise to errors. Therefore, all measurements were made at distances less than the "acoustical radius" calculated for equal direct and reflected intensity [6]. The largest distances used were therefore limited to 75 cm.

Presence of the screen

Disturbance of the sound field due to the presence of the screen was checked by comparing the sound pressure level with and without the screen. Two screens were used for this purpose, one was made of compressed wood fibres (Hard Pavatex 6 mm), smooth and bare, with a very low absorption coefficient (less than 0,2), and the other was covered with a highly absorbing glass-wool (Vetroflex PS 20 mm, absorption coefficient approx. 1 [1]). For experiments for the last two cases acrylic

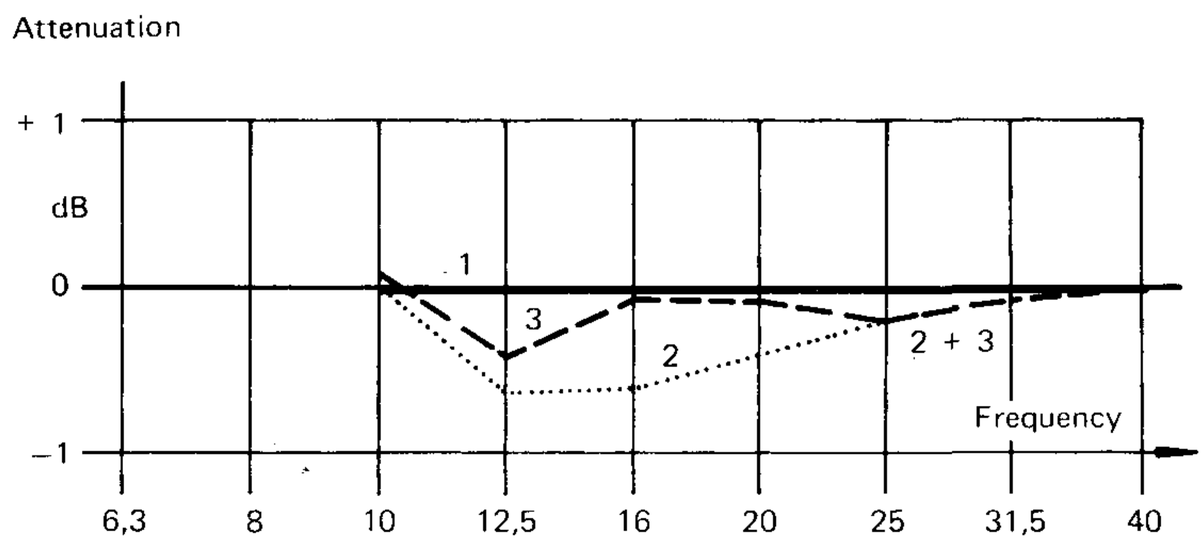

Fig. 2. Absorption influence for a = 5 cm and b = 10 cm (1/2" microphone)
1. without screen
2. with a reflecting screen
3. with a screen made absorbant on the source side

glass screens were used (Plexiglass 5 mm), the measurements show a small disturbance on the transmission side of the sound field close to the screen. However, as soon as the receiver is placed above the screen, making an angle of a few degrees with the x axis, no disturbance is experienced any longer. The results are given in Fig.2.

Air absorption

Finally, decrease in sound intensity was measured as a function of distance, and it was found that the absorption by air is negligible for distances (a + b) less than 1 m. Temperature in the test room was 20 to 22°C, relative humidity being 40 to 50%. In such conditions, absorption by air is 0,4 dB/m at 20 kHz. Considering the short distances used, the absolute error was never greater than 0,5 dB even at 40 kHz. Our measurements being mainly comparative, absorption by air may be neglected.

Measurements with an infinite screen

As previously stated, measurements were taken in the plane limiting the geometrical shadow. Source and transducer could be moved along the x axis, perpendicular to the screen. a was varied from 2,5 to 25 cm and b

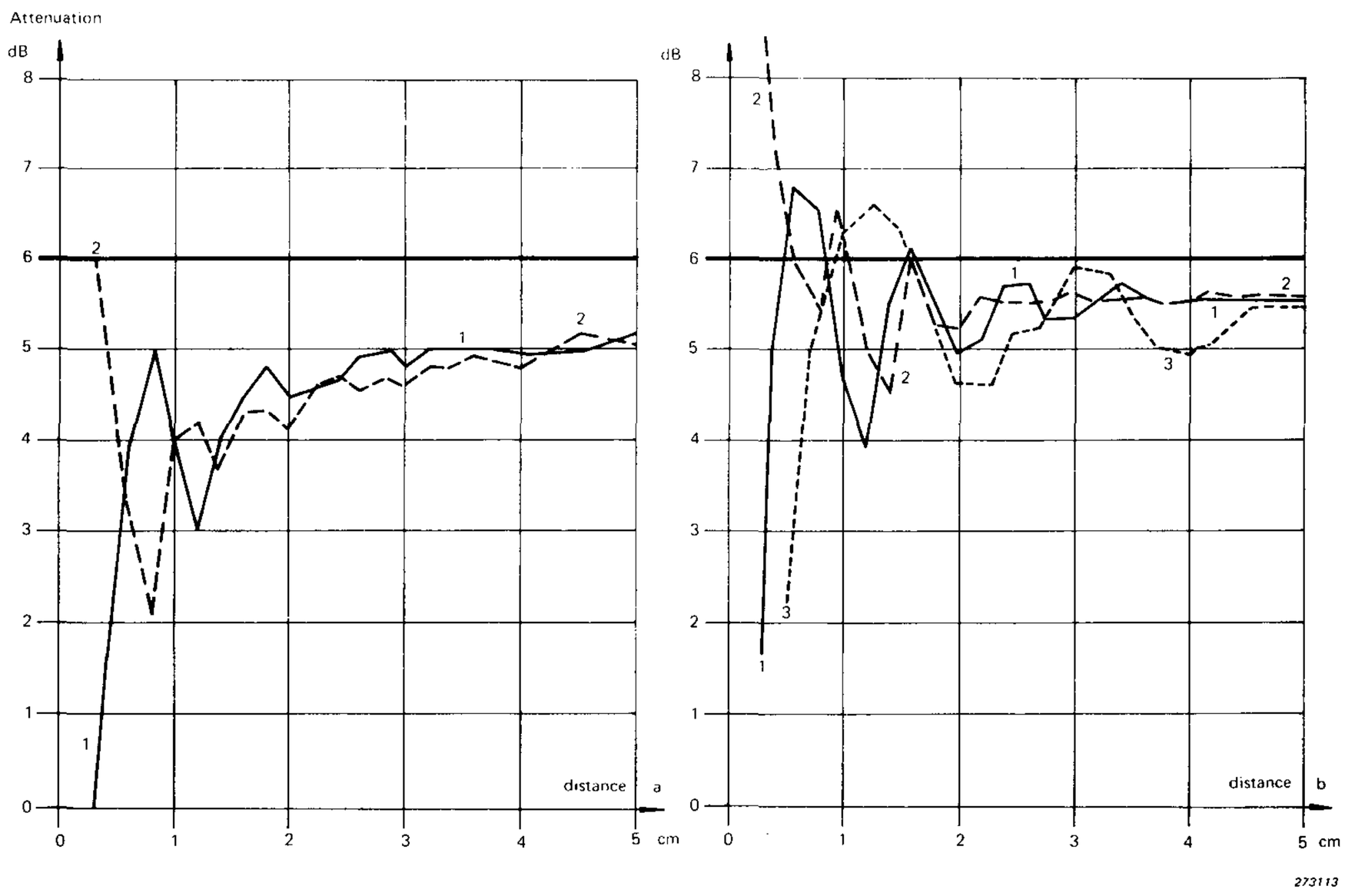

Fig.3a. Field variation in the near field of an "infinite" screen (b = 5 cm)
1. frequency = 20 kHz, 1/2" microphone
2. frequency = 31,5 kHz, 1/2" microphone

Fig.3b. Field variation in the near field of an "infinite" screen (a = 10 cm)
1. frequency = 20 kHz, 1/2" microphone
2. frequency = 31,5 kHz, 1/2" microphone
3. frequency = 10 kHz, 1" microphone

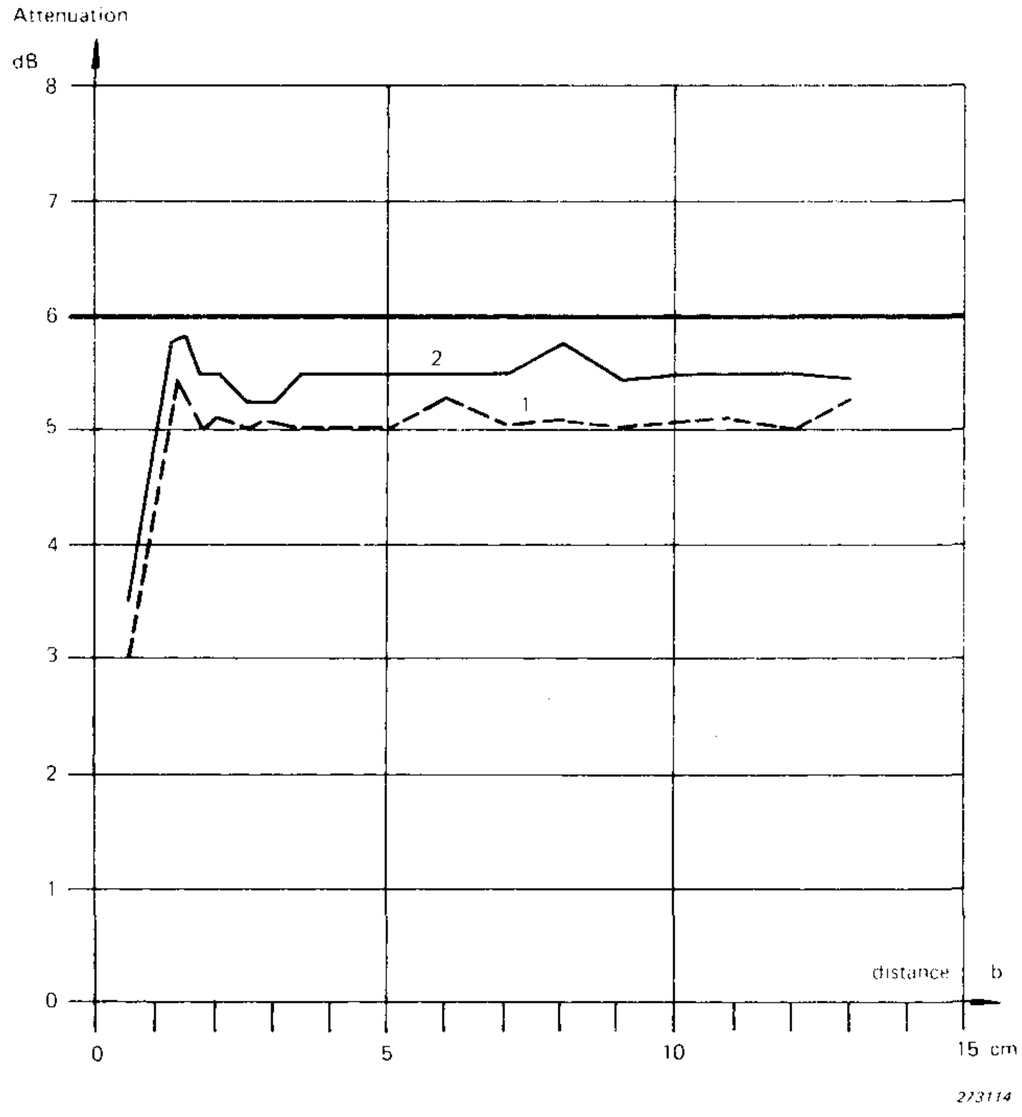

Fig.4. Absorption influence for an "infinite" screen at 10 kHz with a 1/2" microphone a = 10 cm
1. Reflecting screen
2. Absorbing screen

from 5 to 50 cm. The screen length was chosen so that no error due to refraction on the side edges was possible.

The results are given in Figs. 3, 4 and 5. The 6 dB ordinate value which is the theoretical value at the shadow limit [2] is underlined on all figures. A decrease of the sound pressure level is equivalent to the screen attenuation. The screen efficiency is therefore given by the attenuation in dB, as shown on the ordinate axis.

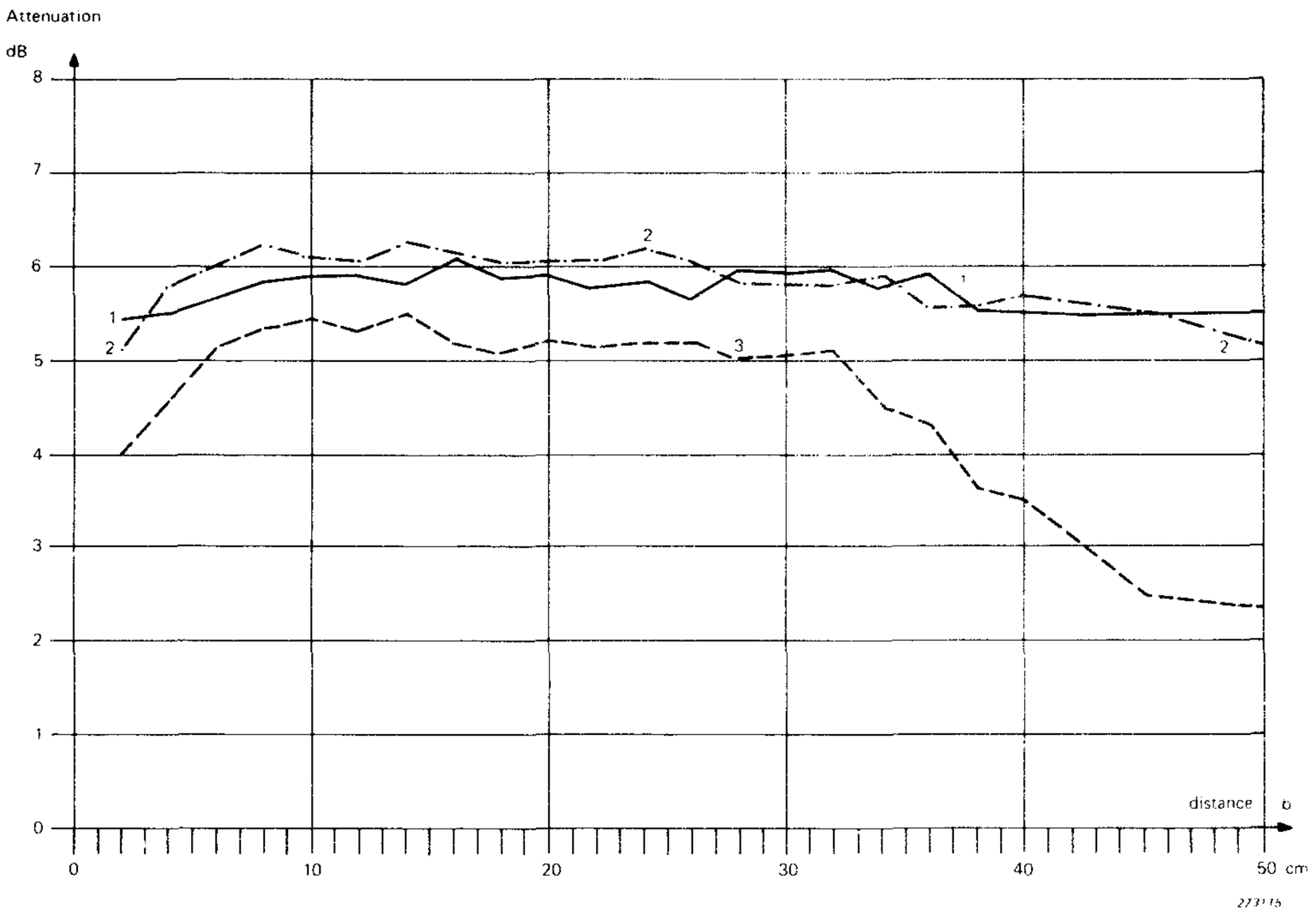

Fig.5. Field variation in the near field with a 1/2" microphone as receiver and a 4 cm loudspeaker as source. a = 25 cm
1. Frequency = 10 kHz
2. Frequency = 5 kHz
3. Frequency = 2 kHz

Measurements on a finite screen

In a similar way, measurements were carried out on a short screen (total length between 6 and 15 cm). The source and the transducer positions were fixed relative to the edge of the screen: a = 5 cm and b = 10 cm, and the source-transducer combination could be moved parallel to the screen edge. As the interest was mainly in the relationship between finite and infinite screens, results given here, taken from 27 experiments, are only related to this relationship.

Fig.6 shows the measured attenuation with four typical screen positions relative to source-transducer positions.

Discussion of the results

It is known from optics that attenuation by an "infinite" straight screen can be calculated using Fresnal integrals.

For the validity of this calculation, the following conditions must be fulfilled.

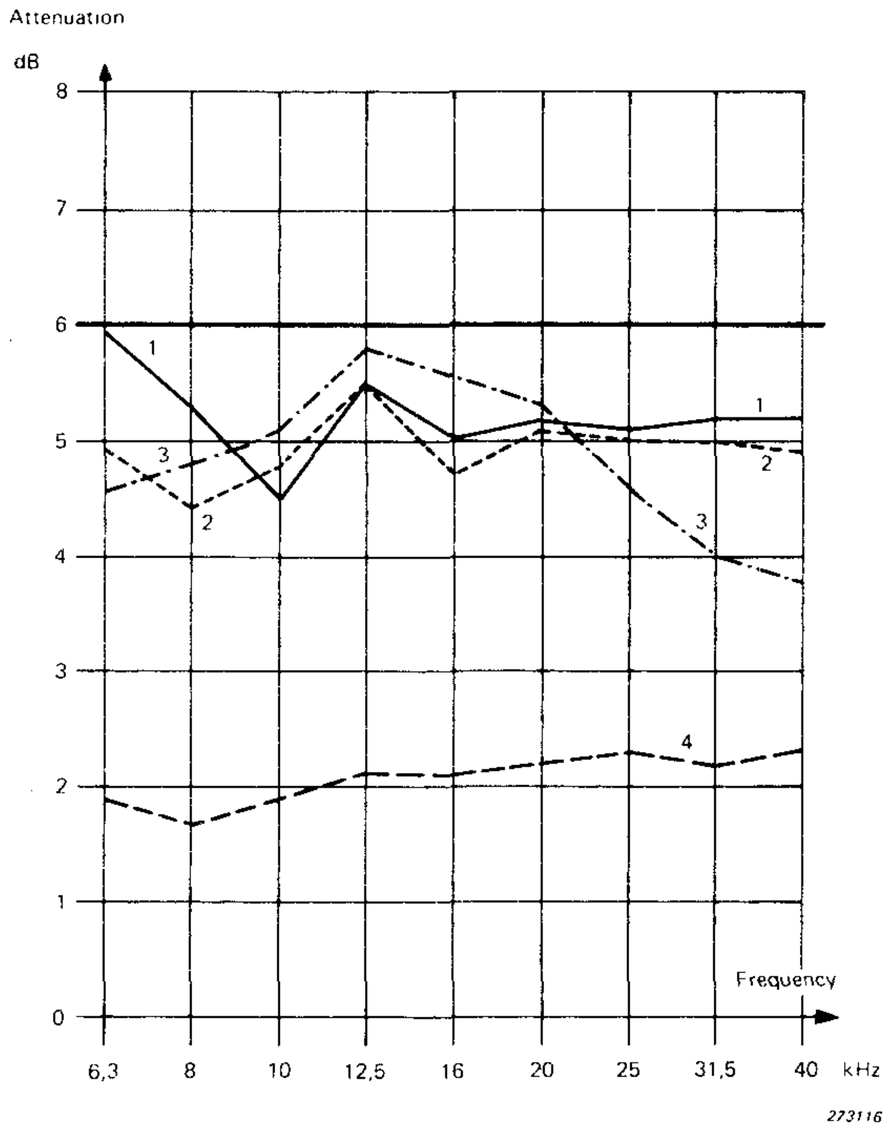

Fig. 6. Field variation in the near field for a "finite" screen. a = 5 cm, b = 10 cm Plexiglass screen, L = 15 cm, 1/2" microphone
Protrusion:
1. 7,5 cm (y = 0 cm)
2. 5,5 cm (y = 2 cm)
3. 2,5 cm (y = 5 cm)
4. 0 cm (y = 7,5 cm)

1. The transmitter is considered to be point-source
2. the ratio d/b is small (see Fig. 7)
3. the observer is not close to the screen

At the geometric shadow limit, intensity is decreased in the ratio:

$$\frac{I}{I_o} = \frac{1}{4}$$

where
I_o = intensity measured without the screen
I = intensity measured with the screen

In terms of sound pressure level, this would mean a reduction of 6 dB.

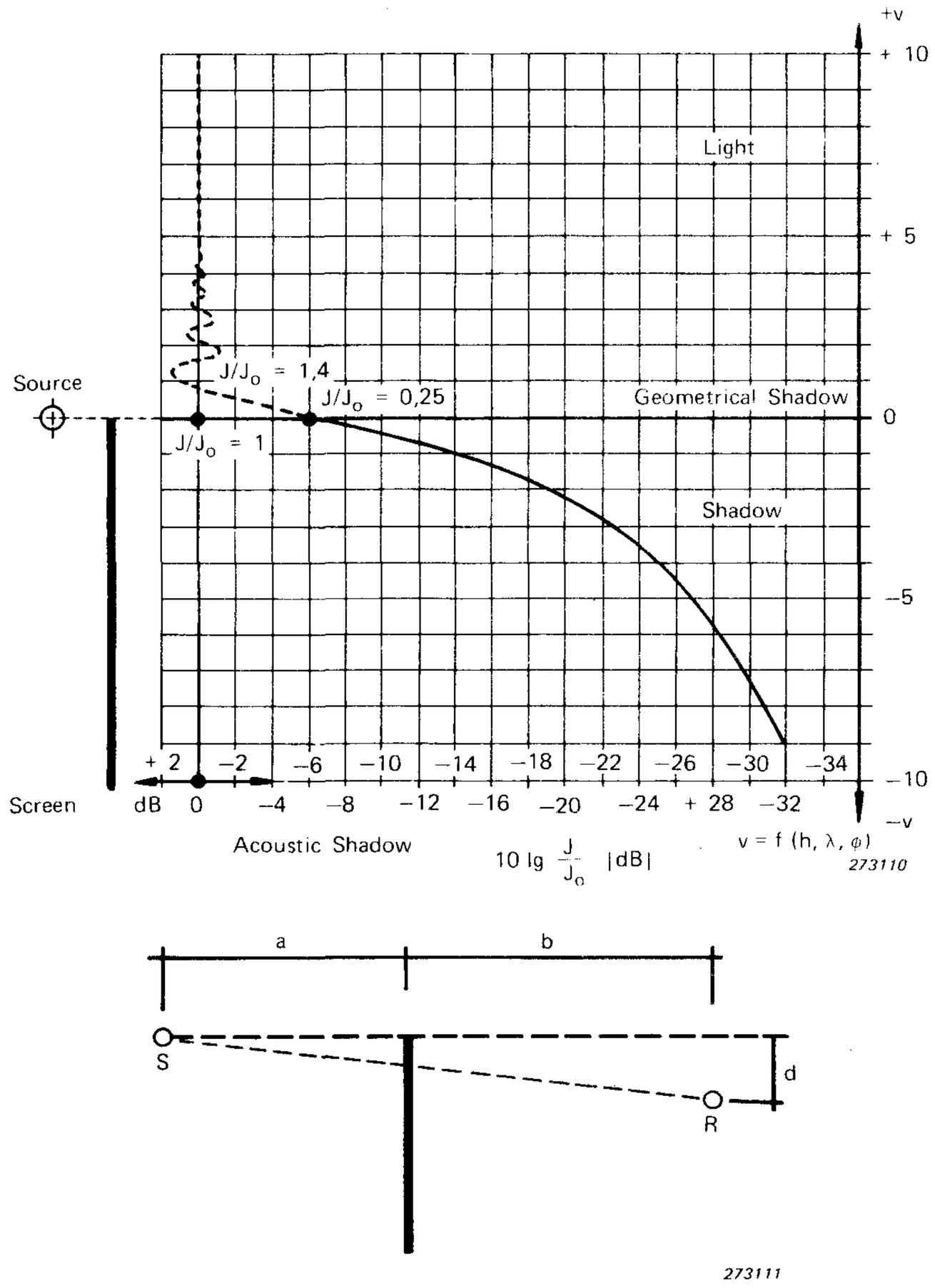

Fig.7. Field intensity behind the screen for the given geometrical repartition

In the case of a straight screen, it showed that the measuring set-up for the model gives results in accordance with the theory. Also the problems of the near-field were considered.

The measuring set-up is meant to simulate noises such as traffic noise and therefore it is basically different from the ideal source on which the screen theory is based. The differences are as follows.

a) the model source is not a point source
b) it is not spherical
c) it transmits a white noise covering the audio range, an octave or a 1/3 octave, but does not produce pure tones.

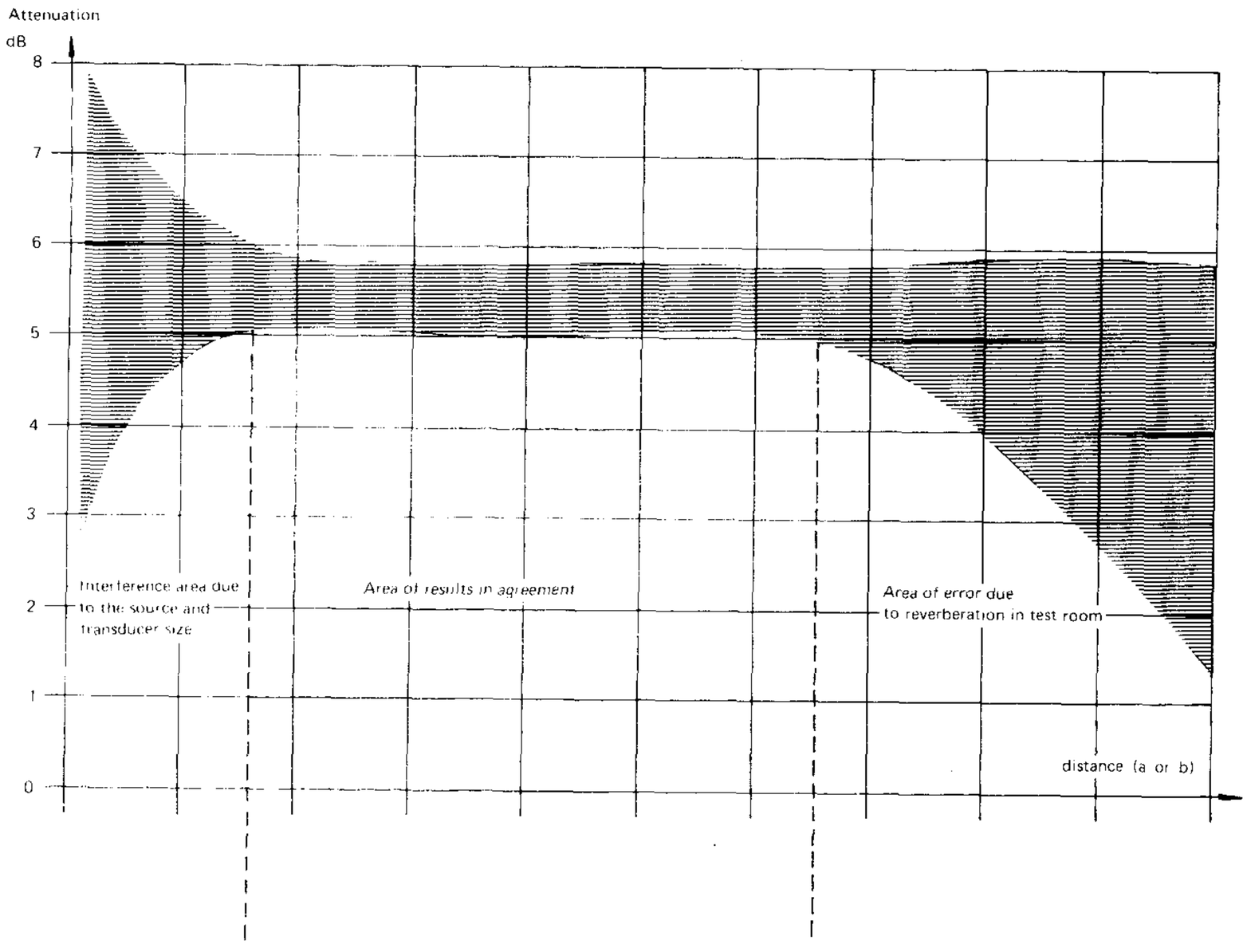

Fig.8. Near field variations for an infinite screen

In spite of these differences, the measurements are close to the values that are predicted by the diffraction theory. Also, the measuring set-up is found to be well suited for model investigations, for example with scale ratios of 1/50 or 1/100 which is very important for traffic noise nuisance study. A general view of the results is given in Fig.8.

Conclusion

a) The preliminary experiments made it possible to check and adjust the measuring set-up as well as to measure the influence of the screen on the sound field of the source. The differences noted between a hard screen and a screen covered with absorbing material on the source side are small. They appear as a reduction of the reflecting screen efficiency as the sound pressure near the screen is increased. For the different measurements, this reduction was found to be always less than 0,6 dB (see Fig.2 and 4).

b) For the long ("infinite") screen, the conclusions may be summarized as follows:

— attenuation due to the screen lies between 5 and 6 dB
— Important interferences appear to be very near the screen and are independent of wavelength (see Figs.3b and 4)

This phenomenon seems to be related to the size of the source and that of the transducer. The limit is approx. 2,5 cm with a 1/2" microphone (source and transducer) and approx. 5 cm with a 1" microphone.

At greater distances from the screen, the limit is determined by the source power and by residual reverberation in the room (see Fig.5), the latter appearing at low frequencies, especially below 10 kHz. Reverberation measurements have corroborated this point. However, satisfactory measurements could be made for distances a + b up to 75 cm.

c) The last series of measurements dealt with short limited screens, which showed that there was a relationship between the wavelength λ and the screen length L. With a protrusion shorter than λ (see Fig.1), a very fast reduction of the screen efficiency is noted. Maximum effect was found with protrusion equal to λ.

If the protrusion is increased, screen efficiency is first slightly reduced and then increases again to be stabilized above 5 dB when the protrusion is over 2λ. This is only approximate since the source size must be taken into account (see curve 3 on Fig.6). If the overlap is further increased interference phenomenon disappears and the normal screen efficiency is obtained. Extension of the screen on either side does not modify the result. No important differences were noted between short symmetrical and asymetrical screens. (see Fig.6).

It is seen from the experiments that the screen has the efficiency predicted by the optics theory even if the source or the observer are placed near the screen. Experiences of people living in the vicinity of high traffic roads, often questionned, are thereby corroborated: Even relatively low embankments give protection against noise. In the case of a house near the road, the protection by the screen at the geometrical shadow limit, is equivalent to a doubling of the distance from the road. Field measurements [7] show that noise is decreased by 5 to 6 dB when the distance is doubled. In acoustics, there is a distinction to be made between reduction due to the distance and reduction at the shadow limit due to the screen. Distance modifies the noise spectrum by air absorption of the high frequency components. This is especially true at long distances. A screen on the other hand at the shadow limit, is not selective and reduces all components by the same amount. Having made these conclusions, it seems that a new rule may be added to the rules of the art of construction, and is relatively easy to remember:

> At the limit of the geometrical shadow, noise reduction is equivalent to the effect of doubling the distance as has been shown.

PREVIOUSLY ISSUED NUMBERS OF BRÜEL & KJÆR TECHNICAL REVIEW

(Continued from cover page 2)

4–1970 On the Applicability and Limitations of the Cross-Correlation and Cross-Spectral Density Techniques.

3–1970 On the Frequency Analysis of Mechanical Shocks and Single Impulses.
Important Changes to the Telephone Transmission Measuring System.

2–1970 Measurement of the Complex Modulus of Elasticity of Fibres and Folios.
Automatic Recording-Control System.

1–1970 Acoustic Data Collection and Evaluation with the Aid of a Small Computer.
1/3 Octave Spectrum Readout of Impulse Measurements

4–1969 Real Time Analysis.
Field Calibration of Accelerometers.
The Synchronization of a B & K Level Recorder Type 2305 for Spatial Plotting.

3–1969 Frequency Analysis of Single Pulses.

2–1969 The Free Field and Pressure Calibration of Condenser Microphones using Electrostatic Actuator.
Long Term Stability of Condenser Microphones.
The Free Field Calibration of a Sound Level Meter.
Accelerometer Configurations.
Vibration Monitoring and Warning Systems.

1–1969 The Use of Digital Systems in Acoustical Measurements.
Impulse Noise Measurements.
Low Frequency Measurements Using Capacitive Transducers.
Details in the Construction of a Piezo-electric Microphone.
A New Method in Stroboscopy.

SPECIAL TECHNICAL LITERATURE

As shown on the back cover page Brüel & Kjær publish a variety of technical literature which can be obtained free of charge. The following literature is presently available:

- Mechanical Vibration and Shock Measurements (English, German)
- Acoustic Noise Measurements (English), 2. edition
- Architectural Acoustics (English)
- Power Spectral Density Measurements and Frequency Analysis (English)
- Standards, formulae and charts (English)
- Catalogs (several languages)
- Product Data Sheets (English, German, French, Russian)

Furthermore, back copies of the Technical Review can be supplied as shown in the list above. Older issues may be obtained provided they are still in stock.

PRINTED IN DENMARK • K. LARSEN & SØN A/S • 2860 SØBORG

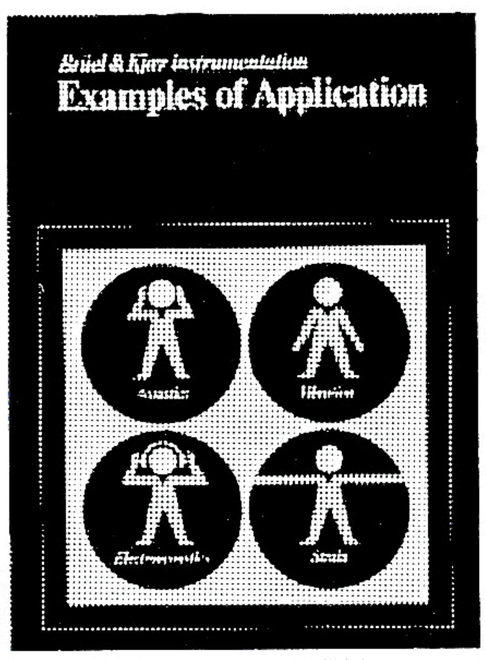

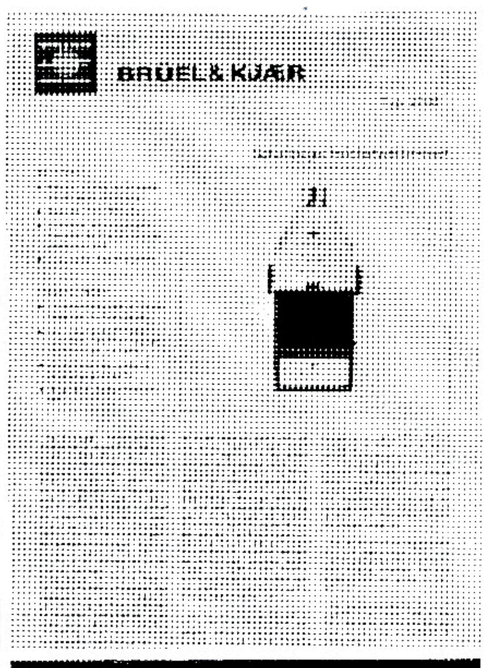

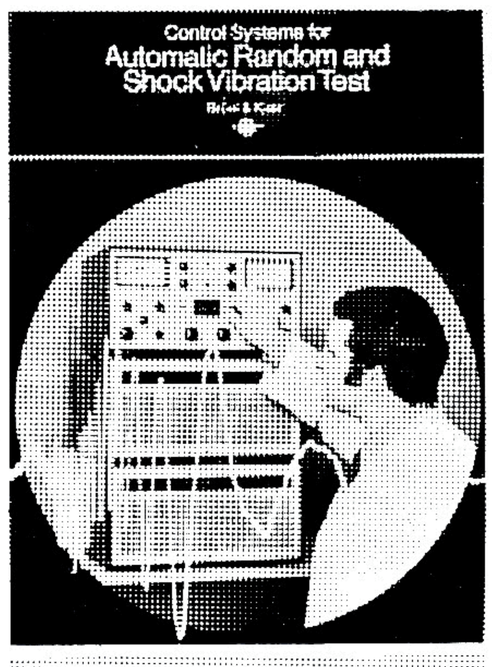

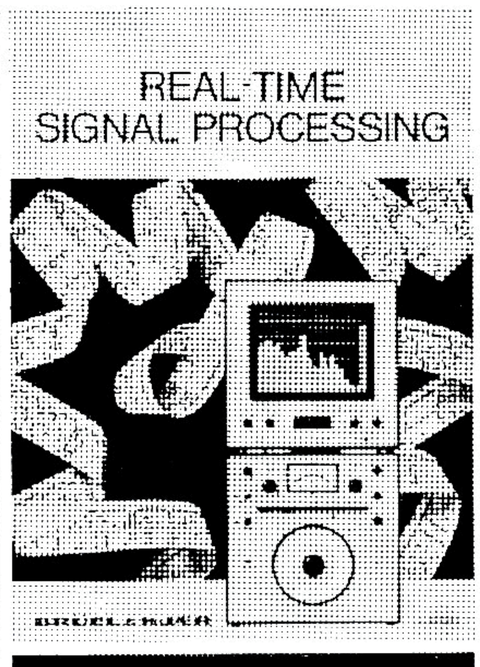

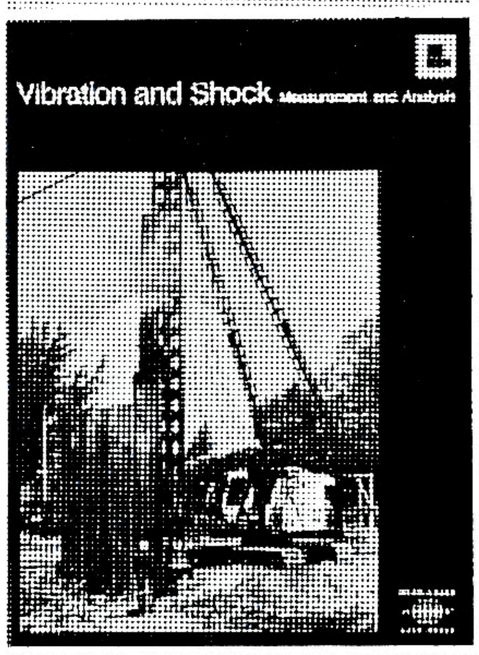

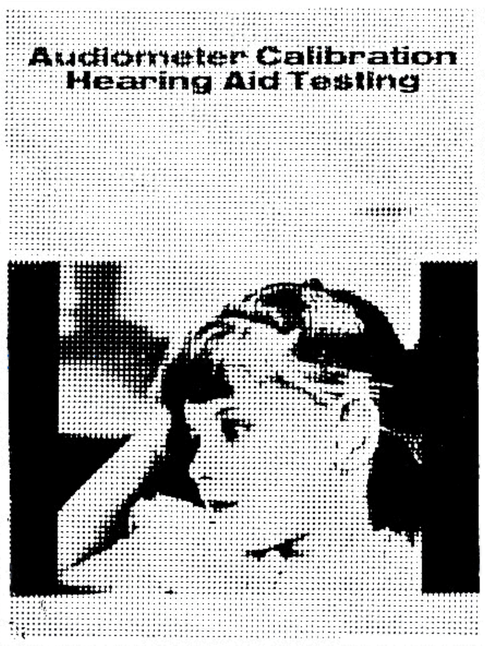

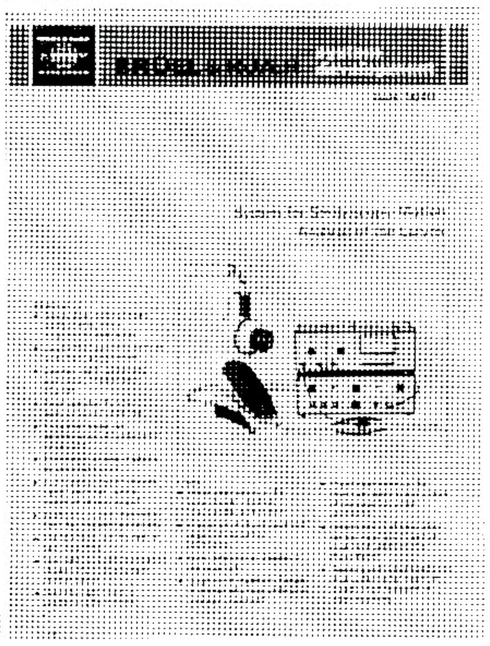

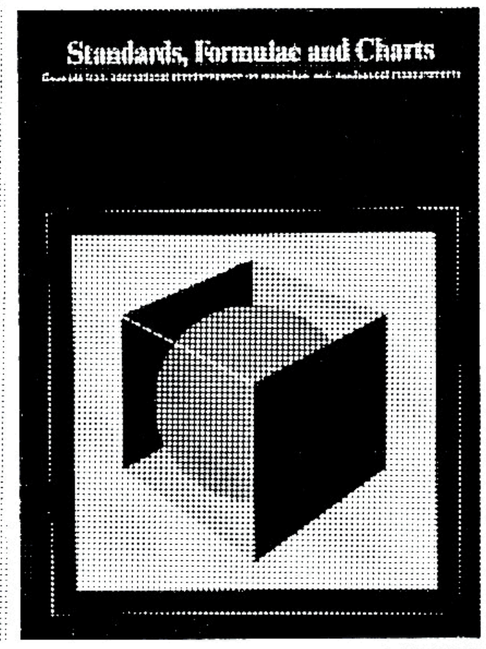

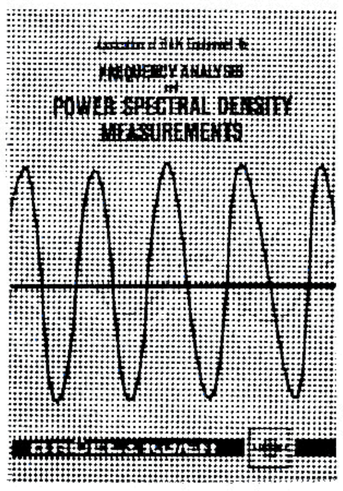

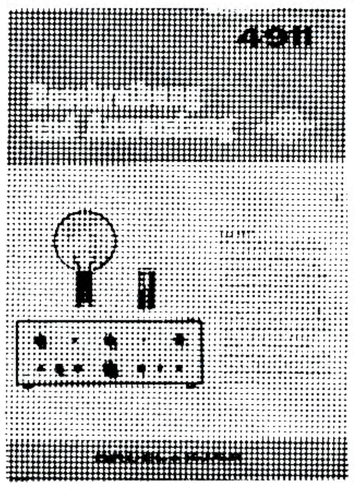

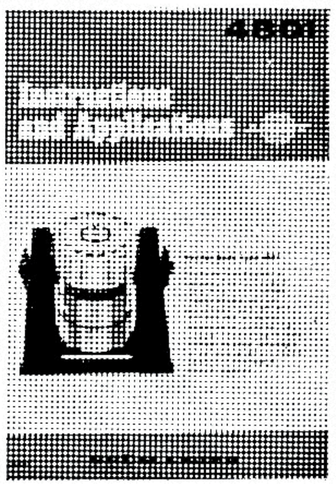

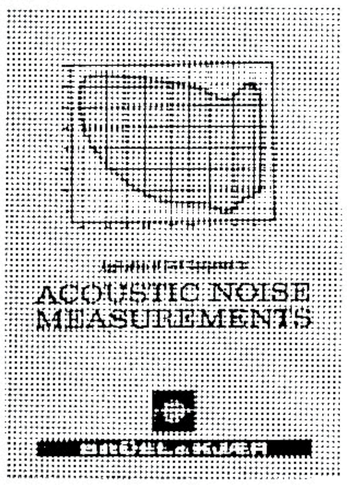

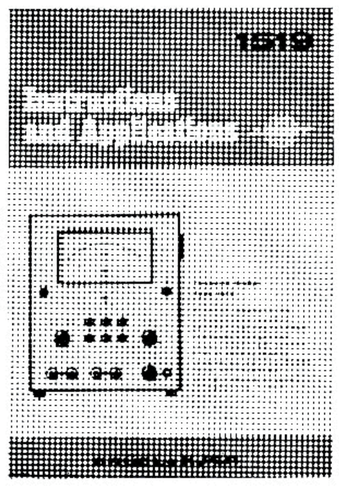

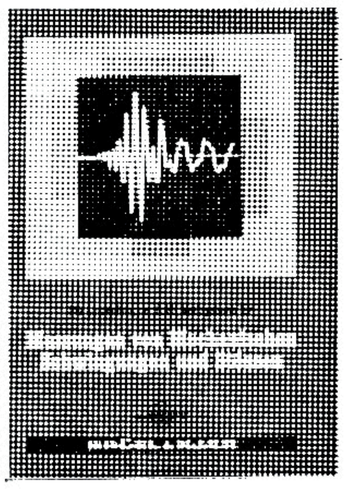

BRÜEL & KJÆR

DK-2850 Nærum, Denmark. Teleph.: (01) 80 05 00. Cable: BRUKJA, Copenhagen. Telex: 15316